metals

MDPI

*Review*

# Titanium Alloy Fabricated by Additive Manufacturing for Medical Applications: Obtaining, Characterization and Application—Review

**Xinjie Zhang, Shuai Liu *, Yude Liu *, Hanjie Guo and Wentian Shi**

School of Artificial Intelligence, Beijing Technology and Business University, Beijing 100048, China
* Correspondence: 20210720@btbu.edu.cn (S.L.); liu_yude@163.com (Y.L.)

**Abstract:** Metal additive manufacturing (metal-AM) technology has made significant progress in the field of biomedicine in recent years. Originally, it was only used as an innovative resource for prototypes. With the development of technology, custom orthopedic implants could be produced for different patients. Titanium alloy is non-toxic and harmless in the human body. It has excellent biocompatibility and can promote the growth and regeneration of bones in its interior. Therefore, it is widely used in the medical industry. However, in the process of additive manufacturing and printing titanium alloys, there are often cases where the powder is not completely melted or the powder adheres to the product structure after printing, which introduces new biological risks. This paper summarizes the causes of powder adhesion from the perspective of the process involved in additive manufacturing, expounds the influence of different processes on the powder adhesion of titanium alloy forming parts, introduces the mainstream methods of powder sticking removal and summarizes the application of the additive manufacturing of titanium alloy in the medical field, which provides a theoretical basis for further development of the application of titanium alloy additive manufacturing technology in the medical industry.

**Keywords:** additive manufacturing; titanium alloy; orthopedic implants; adhering powder; powder removal



**Citation:** Zhang, X.; Liu, S.; Liu, Y.; Guo, H.; Shi, W. Titanium Alloy Fabricated by Additive Manufacturing for Medical Applications: Obtaining, Characterization and Application—Review. *Metals* **2023**, *13*, 462. https://doi.org/10.3390/met13030462

Academic Editors: Takuya Ishimoto and Xuewei Fang

Received: 30 December 2022
Revised: 26 January 2023
Accepted: 19 February 2023
Published: 23 February 2023



## 1. Introduction

Additive manufacturing is a technology based on a digital model, using a digital technology printer as the carrier and metal powder, plastic and other adhesive materials through layered processing and superposition forming to increase the material layer by layer to generate physical items. It is similar to the principle of using ordinary printers to print computer displays in daily life. The difference is that ordinary printers use ink and paper. The additive manufacturing printer uses a special "ink" with different materials such as metal, ceramics, plastics and sand as "printing materials". Through computer control, the materials can be superimposed layer by layer according to the instructions. Then, the plan becomes a real 3D object [1–6]. At present, millions of patients worldwide need artificial joint replacements every year. More than half of the joint implants used in China come from European and American countries. Their design is completely based on the anatomical structure of the western human body, which is quite different from that of Chinese people. The incidence of osteoporosis, arthritis and other musculoskeletal disorders has also increased significantly with the aging of society [7]. Therefore, additive manufacturing is not only in the automotive, aerospace [8] and marine industry [9] areas of application and research. In particular, there has also been a huge development in the medical field. Additionally, its influence is growing. Compared with traditional manufacturing technology, additive manufacturing technology has the advantages of high forming freedom, high speed and better mechanical properties. In the past, orthopedic implants used clinically often had only fixed specifications, which caused the implants on the market to not be fully applicable to every patient. However, it is now possible to use additive manufacturing to customize different implants according to different conditions of patients, which has promoted the development of additive manufacturing technology [10].

Applications in the medical field are mainly divided into pharmaceuticals, orthopedic implants and medical devices. The most used medical additive manufacturing materials are metal alloys, mostly titanium alloys, followed by cobalt–chromium–molybdenum alloys and stainless steel alloys. Due to their low density and association with good mechanical properties, titanium alloys are considered superior compared with other metallic alloys, having a strength/density ratio of about 300–400 MPa, which is higher than of that steel alloys. The common alloying elements in titanium alloys are Mo, Nb, Ta, Sn, Pd, Hf and Zr, which are highly biocompatible alloying elements. They can improve the mechanical properties and plasticity of titanium alloys and reduce the elastic modulus [11,12]. Titanium alloys have the characteristics of high strength, low density, low temperature resistance, corrosion resistance and are non-magnetic [13–36]. Titanium alloy is a non-toxic and harmless alloy, it can resist the corrosion of secretions and it can adapt to a variety of sterilization methods. Therefore, it is widely used in the manufacture of medical devices. The 3D-printed formed parts made of titanium alloy not only have high strength and are loose, porous and very light, but they also have excellent biocompatibility, which can promote the growth and regeneration of bones inside them well, thus greatly improving the effect of implant surgery. Therefore, it is widely used in the manufacture of orthopedic implants [37–40]. However, the hardness and stiffness of metal materials are much greater than those of human bones. Implantation into the human body can easily lead to a stress shielding effect, which will lead to the loosening of substitutes. In order to avoid the phenomenon of stress shielding, orthopedic implants with porous structure can be fabricated by 3D printing technology. On the one hand, the stiffness of bone implants can be adjusted by adjusting porosity. On the other hand, the porous structure is conducive to the growth of tissues around the bone implant, and enhances the effective integration of the bone implant and human tissue through new bone formation, making full use of the advantages of additive manufacturing technology to form complex structures.

Due to the different degree of rapid melting of titanium alloy powder at high temperature and the settlement of molten pool in the process of using additive manufacturing technology, there are often cases where the powder is not completely melted or the powder adheres to the product structure after printing. Many experts [41,42] have found that there is a large amount of powder adhesion inside the titanium alloy's porous structure formed by additive manufacturing. If the products containing these residual powders are implanted in the human body, the residual powders will fall and flow with the blood over time, causing potential safety hazards such as inflammation, and thus introducing new biological risks [43]. There are also many experts [44,45] using different powder removal technology for porous structures. However, it still has problems such as unsatisfactory powder removal effects and difficult powder removal. Therefore, the removal of insoluble particle residues in titanium alloy orthopedic implants by additive manufacturing has become the focus of research, and it is also a problem that every manufacturing enterprise and scientific research institution must face [46]. This paper points out the core problems of additive manufacturing titanium alloy in the development of the medical industry and summarizes the causes of powder adhesion from the perspective of the process involved in additive manufacturing. In this paper, the effects of the three different processes of binder jetting, powder bed fusion and directed energy deposition on titanium alloy forming parts are described. Mainstream methods of powder adhesion removal are introduced, such as ultrasonic cleaning, chemical cleaning, sandblasting, dry ice jet and so on. This paper also summarizes the main applications of additive manufacturing titanium alloys in the medical field, which provides a theoretical basis and reference for the application of titanium alloy orthopedic implants based on additive manufacturing, and promotes its further development.

## 2. Metal Additive Manufacturing Process Used in Medical Treatment

The problem of powder adhesion in additive manufacturing refers to the insoluble metal powder particles left on the surface or inside of the formed part after forming. It mostly occurs in the process of using metal materials and ceramic materials [47]. Cai and other scholars [48] found that there is a large amount of powder adhesion in titanium alloys formed by additive manufacturing. According to the current international standard ASTM F2792-12a [49,50], etc., additive manufacturing can be divided into seven different categories: binder jetting, directed energy deposition, material extrusion, material injection, powder bed fusion, sheet lamination and stereo light curing. The standard pointed out that binder jetting, powder bed fusion and directed energy deposition all produce powder adhesion. At present, scholars [51–53] have found that the optimization of process parameters can eliminate, or at least significantly reduce, the powder adhesion in metal additive manufacturing technology, which confirms that different processes and process parameters are indeed related to powder adhesion. Therefore, I will review the principles and process parameters of binder jetting, powder bed fusion and directed energy deposition.

### 2.1. Binder Jetting

Binder jetting is similar to the composition and process of traditional printers; it was originally called three-dimensional printing (three-dimensional printing, referred to as 3DP) technology [54]. It was proposed by Professor Sachs of Massachusetts Institute of Technology (MIT) in 1993. The ASTM Committee of the United States officially named BJ technology. Since then, China has also paid considerable attention to BJ technology. Some companies, such as Esquel, Fenghua Zhuoli and Ningxia Share, have successively launched BJ printers. The characteristics of high efficiency and low cost make binder jetting technology widely used in the medical field to make denture frames [55] and orthopedic implants [56].

The process of binder jetting is to spread a certain thickness of powder on the substrate and then spray the binder to the powder layer. After one layer is sprayed, the printing platform reduces the height of the layer, and the powder is spread from the powder supply source to the powder bed by the powder spreading roller [57]. The powder bed is accumulated layer by layer to obtain a three-dimensional entity. Binder jetting also has shortcomings; the main ones are as follows: (i) the binder that is added to the metallic powder can be toxic (not biocompatible material), (ii) the sintering process usually changes the shape of the model (shrinking it by about 20%), and the accuracy of the implant shape is essential, (iii) some residual binder can be present (due to the unstable sintering process). If this section refers to medical treatment, it should have information regarding the materials that are used for these technologies, such as alloys and recommended powder size. Due to the above problems, the relevant information such as binder removal and recommended powder size is particularly important. Binder can be divided into organic and inorganic binders according to their composition. In the medical field, non-toxic polyethylene is usually used as a binder. It should be noted that before the post-treatment process of binder jetting, the binder in the initial billet needs to be removed by degreasing and heat treatment to avoid introducing new safety hazards [58]. In recent years, binder jetting printing materials have been continuously expanded from iron-based materials to active metal materials such as titanium alloys, superalloys and even magnesium. It was found that 16~25 μm powder samples have the fastest densification rate [59]. In the process of binder jetting, the interaction between binder and powder bed is very complex. Stevens et al. [60–62] pointed out that there are two stages to introducing residual powder (Figure 1): high-speed impact and the diffusion stage. High-speed impact will lead to the fracture of the powder bed, causing droplets and powder splashing to form adhesive powder, affecting the forming quality. The diffusion through capillary action may lead to residual powder at the edge. These adhered excess powders affect roughness and dimensional accuracy.

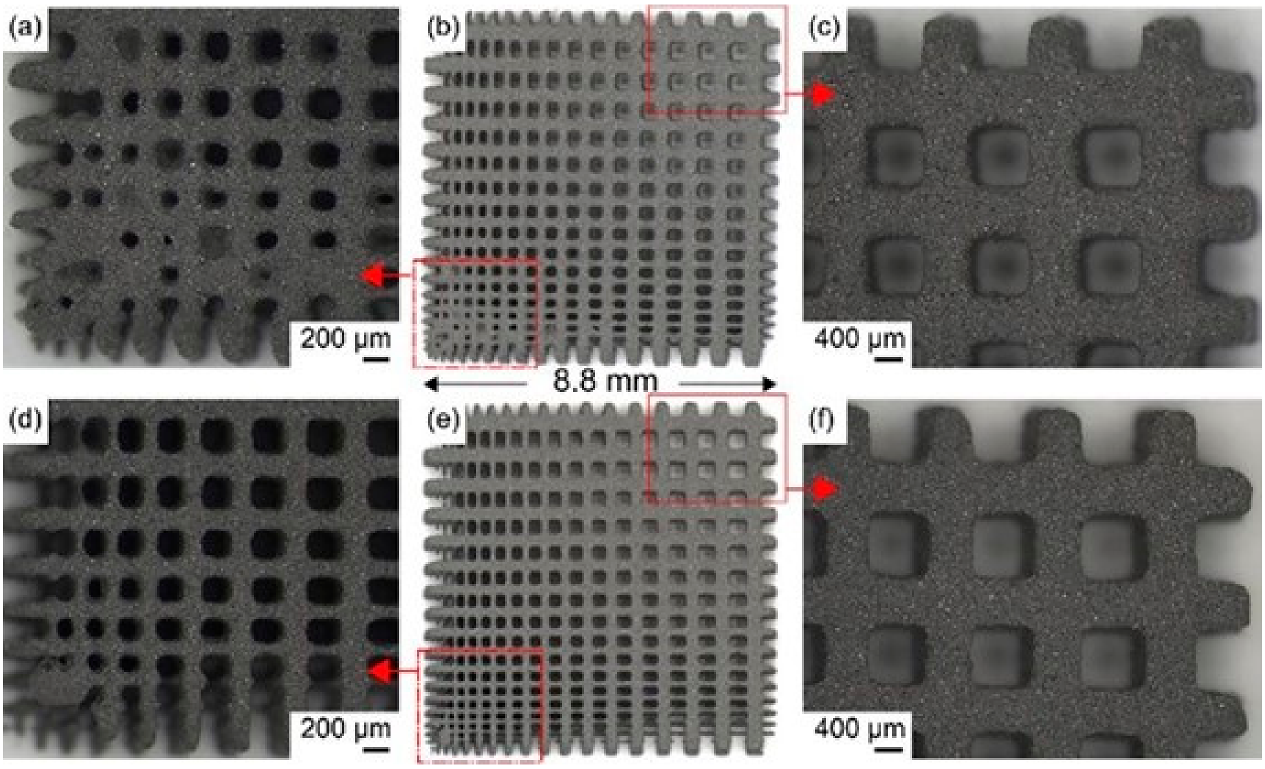


**Figure 1.** Adhesive powder for molded parts printed using binder jetting. Reprinted with permission from Ref. [62]. Copyright 2015, copyright Jurisch M, Studnitzky T, Andersen O. Comparison of formed parts based on two different binder: B1(**a**–**c**) and B2 (**d**–**f**).

It can be seen that the residual powder is usually introduced in the high-speed impact and diffusion stages during the binder jetting process. Chen and Zhao [63] found that the degree of defects and surface finish can be improved by adjusting the process parameters in the binder spray manufacturing process, such as layer thickness, binder saturation, powder spreading speed and so on. On the one hand, the forming process is carried out on the powder bed, so the thickness of the powder layer will directly affect the transport and conduction of the binder, resulting in defects such as uneven bonding of the powder [64]. On the other hand, the amount of binder at low saturation is small, and the powder cannot be firmly bonded together. The powder may fall off to form a binder, while the binder at high saturation will cause excessive powder to bond to the surface and increase the surface roughness [65]. Some scholars [66] have found that when the layer thickness, powder spreading speed and powder feeding ratio are 100 μm, 6 mm/s and 3:1, respectively, and there is 70% binder saturation, the adhering powder defect can be effectively improved. However, there is still a lack of in-depth research on the powder spreading speed, which needs to be further expanded.

### 2.2. Powder Bed Fusion

Powder bed fusion technology is one of the popular manufacturing methods under metal additive manufacturing technology, first developed in 1994 [67]. The characteristics of flexible design and highly efficient utilization of resources have enabled it to be applied in the biomedical industry [68]. It was first used in the medical field to manufacture jaws and teeth [69,70]. The powder bed fusion technology is divided into selective laser melting (SLM) and electron beam melting (EBM). The forming schematic diagram is shown in Figures 2 and 3. These two technologies not only have high forming efficiency and accuracy, but also have a wide range of applications. These advantages also highlight the potential of SLM and EBM to directly manufacture orthopedic implants [71–73].

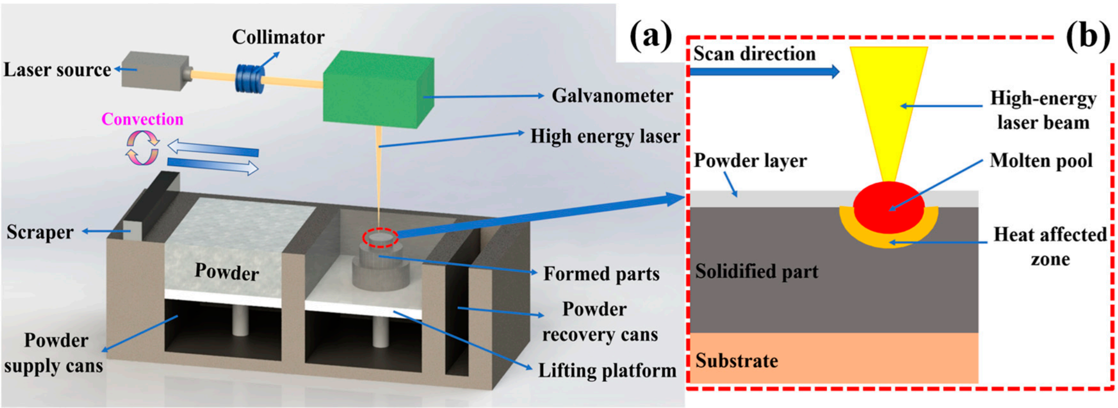


**Figure 2.** The SLM equipment and forming schematic diagram: (**a**) the equipment of SLM; (**b**) the schematic diagram of SLM. Reprinted with permission from Ref. [70]. Copyright 2022, copyright Shi W, Li J, Liu Y.

The powder bed fusion technology is to use laser or electron beam to irradiate the whole powder layer, heat the powder to the melting point of the forming material and selectively fuse the powder layer. After that, one lowers the forming platform and lays a new layer of powder in the forming area. The powder layer is continuously heated and selectively fused layer by layer, and finally the formed part is obtained. The processing of powder bed fusion includes two steps: firstly, the powder melts after receiving heat; secondly, the liquid metal solidifies on the substrate or precursor layer. The second step is the uniform wetting process. Uniform wetting is the main mechanism of melt wetting on similar material substrates [74]. This is a non-equilibrium process including fluid flow, heat conduction and solidification [75]. In this process, gravity and capillary force cause the molten pool to settle, and if the temperature of the molten pool is too high, the droplets splash and adhere to the unmelted powder, which makes it impossible to avoid the introduction of residual powder and produce powder adhesion defects.

It is shown that the powder adhesion defects can be improved by adjusting the energy density (Figure 4). The results show that for Ti-6Al-4V titanium alloy powder, the surface of the sample is flat, the forming accuracy is high and the powder adhesion is at its least when the energy density of forming parts is 150~170 J/mm$^3$ [76–80]. Therefore, the powder bed fusion process is an important factor affecting the powder bonding performance. Laser energy density directly affects the viscosity and fluidity of the molten pool, thus directly affecting the fusion between different powders. When the laser beam hits the powder, a series of physical and chemical changes occur after the powder particles are heated. The powder is heated and melted to undergo a phase transition. At this time, the spreading and solidification of the melt are carried out at the same time. When the spreading speed of the melt is faster than the solidification speed, a smooth and flat surface is formed. On the contrary, it causes defects such as adhering powder and spheroidization. Therefore, mastering the exact laser energy input and controlling the spreading and solidification process of the melt directly affects the final forming quality. When the laser energy density of the formed Ti-6Al-4V titanium alloy is too high (170~250 J/mm$^3$), the amount of powder splashing increases, and a large amount of powder is attached. When the laser energy density is too low (0~80 J/mm$^3$), the melting is not complete and the spheroidization increases [81,82]. Non-toxic biocompatible elements and Ti are often added to form titanium alloys, such as TiNb and NiTi titanium alloys [83]. By studying the NiTi titanium alloy formed by SLM, it is found that when the laser energy density (55.56–66.67 J/mm$^3$) is used, the powder particles are fully melted and the solid powder rarely adheres to the surface of the deposition layer. As shown in Figure 5, there are no cracks and other defects inside, only spherical pores with dispersed distribution. When a sufficient energy density (65~80 J/mm$^3$) is input, all NiTi titanium alloy powder particles melt and avoid spheroidization [84]. In summary, the optimal laser energy density range should be adopted for the titanium alloy powder, and the optimal energy density required for different titanium alloy powders is different. It is necessary to determine the theoretical optimal temperature through the thermodynamic and kinetic theoretical calculation of the melt with specific composition so as to control the powder adhesion.

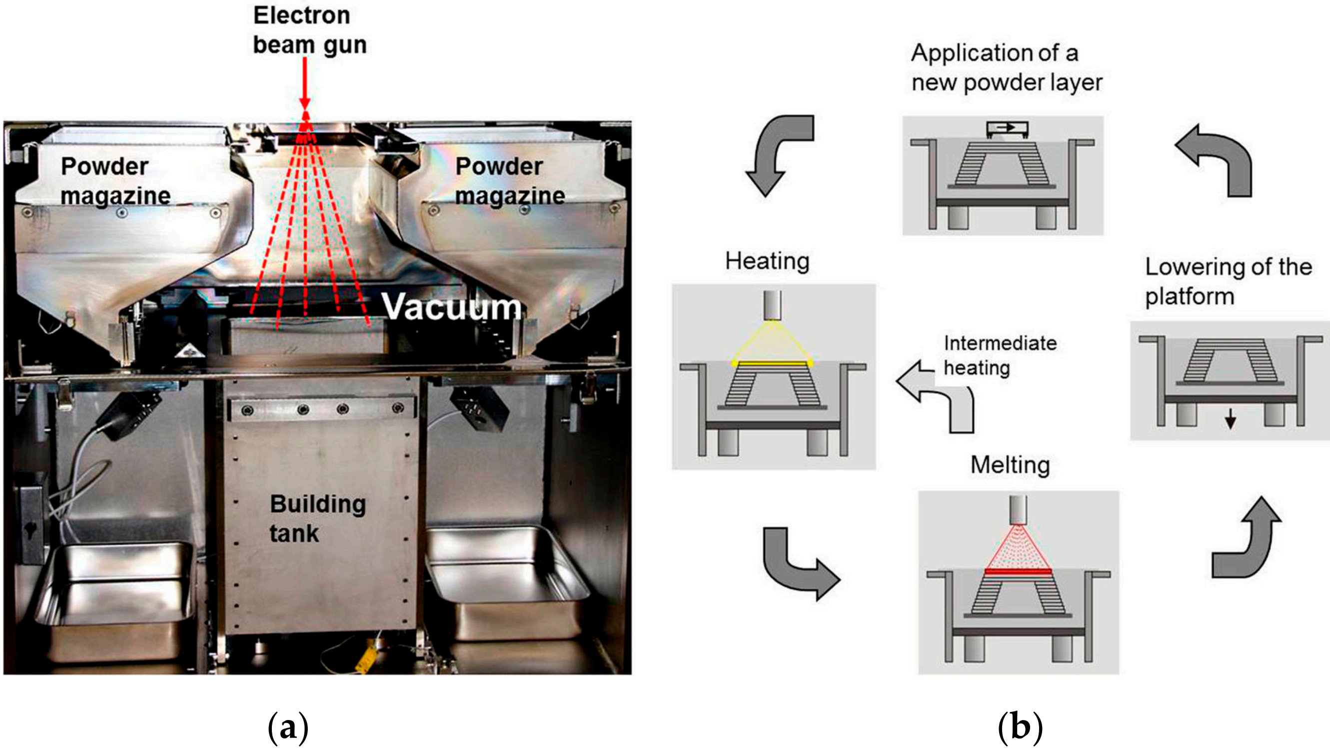


**Figure 3.** The EBM equipment and forming schematic diagram: (**a**) the equipment of EBM; (**b**) 4-step process for building one layer. Reprinted with permission from Ref. [81]. Copyright 2016, copyright Körner C.

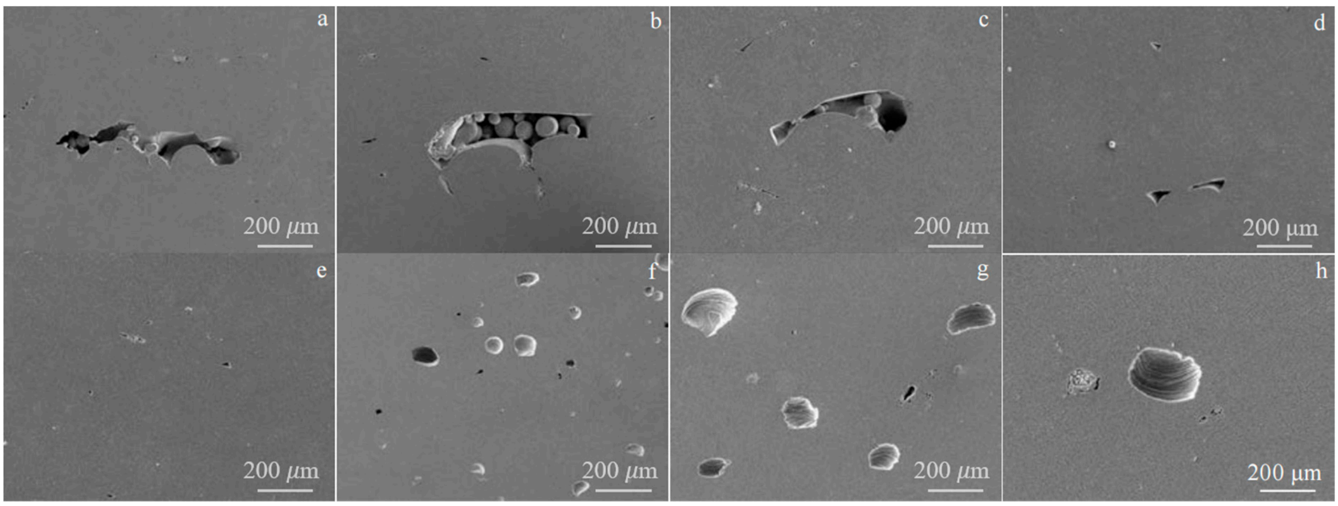


**Figure 4.** Diagram for defects evolution with laser energy density of 27 J/mm$^3$ (**a**), 33 J/mm$^3$ (**b**), 44 J/mm$^3$ (**c**), 58 J/mm$^3$ (**d**), 98 J/mm$^3$ (**e**), 213 J/mm$^3$ (**f**), 253 J/mm$^3$ (**g**) and 333 J/mm$^3$ (**h**). Reprinted with permission from Ref. [71]. Copyright 2021, copyright Zhao C, Li W, Wang Q, Wang Y, Zhao Y, Di S, Ren D, Ji H.

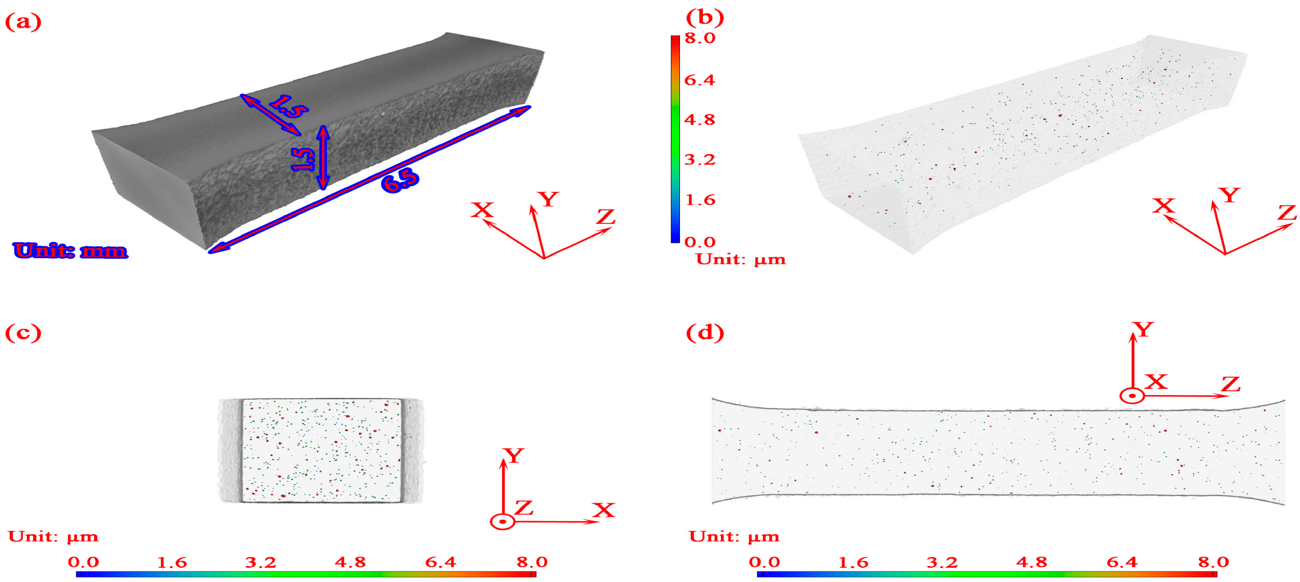


**Figure 5.** Three-dimensional reconstruction graphs showing the internal defect distribution within the M-VED NiTi sample: (**a**) selected scanning region, (**b**) axonometric drawing, (**c**) side view, (**d**) front view. Reprinted with permission from Ref. [84]. Copyright 2022, copyright Ge J, Yuan B, Zhao L.

*2.3. Directed Energy Deposition*

Directed energy deposition technology was invented in 1996 at the Sandia National Laboratory in the United States. Its advantages include high forming precision, fast speed and small processing size limit [85–87]. In the medical field, it is often used to coat the surface of medical implants produced by traditional processes to achieve a porous structure on the surface of implants, which is conducive to bone growth [88,89].

Laser beams, electron beams or plasma are used as high temperature heat sources to melt the surface of the substrate to produce a molten pool. The raw materials are synchronously fed into the molten pool through the feeding equipment. The raw materials are solidified after rapid melting and cooling and form a metallurgical bond with the matrix material. In this process of high temperature and rapid cooling, defects such as incompletely melted powder adhering to the surface of the formed part will inevitably occur, resulting in the powder defects of [90–93].

The research shows that the optimization of the process parameters of the directed energy deposition technology can reduce the surface roughness of the formed parts and improve the adhering powder defects. The typical process parameters of the directed energy deposition technology such as laser power and powder feeding rate affect the powder adhesion in the forming process (Figure 6). Therefore, it is also very important to understand the process parameters in the directed energy deposition technology. On the one hand, the larger the laser power, the wider and higher the cladding layer and the larger the molten pool. The reason is that the heat input increases, which leads to the increase in the temperature rise in the powder air and the ability of the molten pool to melt the powder. On the other hand, the larger the powder feeding rate, the wider and higher the cladding layer but the smaller the penetration of the substrate. The reason is that the energy absorption ratio of the powder substrate increases, which leads to the increase in the powder melting amount, which is beneficial to improve the utilization rate of laser energy and reduce the adhering powder [94–97].

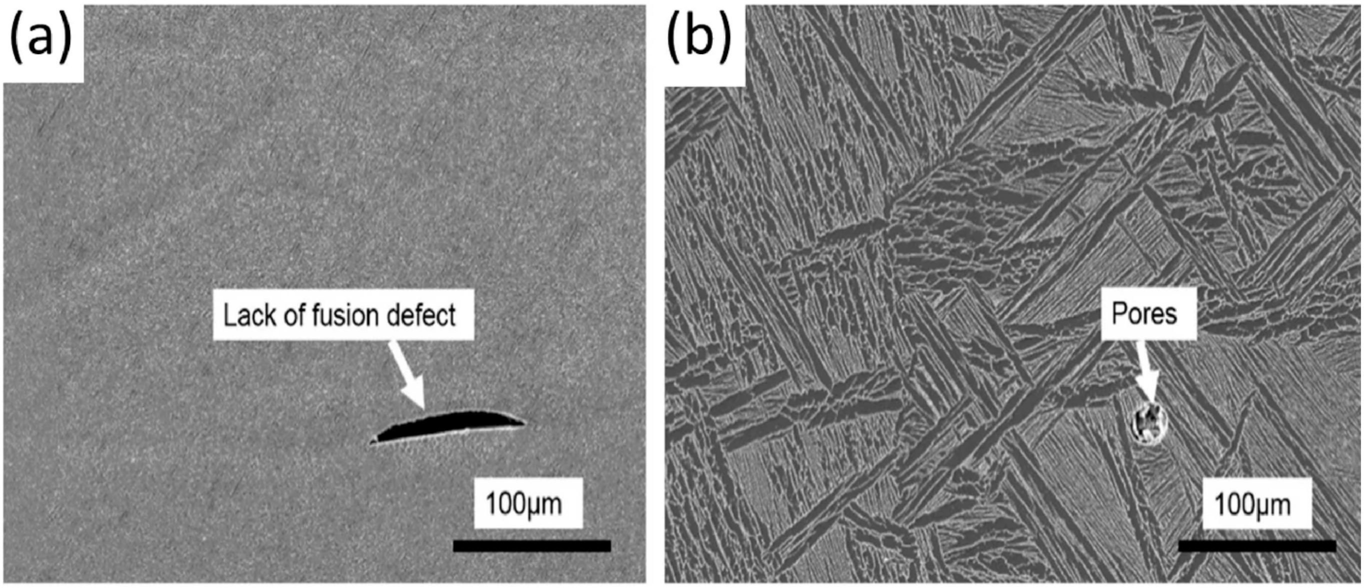


**Figure 6.** Directional energy forming Ti-6Al-2Zr-2Sn-3Mo-1Cr-2Nb forming parts defects (**a**) unmelted powder (**b**) porosity. Reprinted with permission from Ref. [90]. Copyright 2021, copyright Liu Z, He B, Lyu T, Zou Y.

## 3. Key Issues of Titanium Alloys in Medical Additive Manufacturing

### 3.1. Cause of Powder Adhesion

The application of additive manufacturing technology in the medical field has realized the complex structural design of orthopedic implant devices, such as porous structure and anatomical site matching, which provides a new choice for the production process of orthopedic implant devices [98,99]. It must have mechanical properties that meet the requirements of natural human bone parameters, including compressive strength, strain and elastic modulus [100]. For example, most of the mechanical properties of solid metals are higher than those of natural human bone. At the same time, it will lead to mismatched parameters and the problem of stress shielding [101]. Later, experts found that the mechanical properties of orthopedic implants can be reduced by changing the structure and adjusting the relative density, so as to meet the requirements for implantation in the human body [102–105]. Secondly, it should have good bio-functionality. Considering the adaptability of the implant to bone after implantation, the metal material of the implant should have sufficient biocompatibility to ensure no rejection after implantation. Surface polishing can not only reduce the surface roughness of orthopedic implants and reduce friction, but also improve cell adhesion and osteogenic ability [106]. The common methods of orthopedic implants include mechanical polishing [107], chemical polishing [108] and fluid polishing [109]. In addition, the final cleaning process of the implant is to ensure the safety of the implant. As mentioned above, three different processes in additive manufacturing technology produce adhering powder. This directly affects the bio-functionality. The high-speed impact and diffusion in the binder jetting process, the increase or settlement of the molten pool in the powder bed fusion process and the rapid heat input in the directed energy deposition process are all causes of powder adhesion. In additive manufacturing, a thin powder layer is laid and selectively melted or bonded layer by layer to construct a component. In this process, a reaction of high temperature and rapid cooling occurs, or laser high-speed impact and so on [110]. The metal powder diffuses to form a uniform layer before selective melting using a melting or suitable liquid binder. Due to the small size of the powder near the melting zone and the capillary action of the adhesive liquid, the adhesion of fine powder to the contour of the component is inevitable. In the process of layer-by-layer construction, the heat dissipation part of the laser source melts the powder around the contour edge, resulting in the phenomenon of the adhering powder [111]. This disadvantage caused by additive manufacturing technology also affects the bio-functionality of orthopedic implants. By implanting the SLM-formed titanium alloy bone scaffold into the femur of the knee joint of the small Xiang pig's hind leg for 30 days, Fan found that the scaffold with no residual powder after post-processing and conforming to the bionic bone structure had good biocompatibility, and there was no inflammation and infection in the surrounding tissue after implantation. In contrast, inflammation was found in the wound of the piglet 3 days after implantation in the bone scaffold control group with residual powder [112]. Therefore, the residual powder causes low forming quality and large surface porosity, which is not conducive to cell adhesion. The bad thing is that once the adhering powder falls off after implantation, it has an adverse effect on the human body. After processing, it is necessary to remove the residual powder to ensure the forming quality of the implant and avoid adverse reactions after implantation [113].

Residual powder refers to the insoluble metal powder particles left in the manufacturing parts after the forming is completed. The adhesion of residual powder is the key problem in the medical additive manufacturing of titanium alloy. For the removal of residual powder, scholars [114] have found that the use of ultrasonic and sandblasting methods can remove and improve the forming quality of the implant. For example, Zebrowski et al. [115] used sandblasting to modify the surface of the implant and explored the modification effect under different working pressures. The results showed that sandblasting can remove the residual powder of the implant, promote osseointegration and reduce the risk of bacterial infection and surgical complications. In addition, as a new surface modification technology, acoustic surface modification technology is safe, simple and effective. It can improve surface quality and reduce surface porosity without contact [116]. In medical additive manufacturing, any loose powder trapped in the pores of orthopedic implants and powder adhered to the surface may be discharged into the body, causing inflammation or blocking blood vessels. It is very important to master the method of removing adhering powder.

## *3.2. Adhering Powder Removal Method*

### 3.2.1. Ultrasonic Cleaning

Ultrasonic cleaning is the use of ultrasonic cavitation in the liquid, accelerating the effect and the role of direct flow, in order to overcome the adhesion of particles. Ultrasonic cleaning can disperse and peel the residual metal powder from the surface of the sample and the interior of the pore structure so as to achieve the purpose of cleaning. As summarized in Table 1, the advantages and disadvantages of ultrasonic cleaning are that the ultrasonic wave has high frequency, short wavelength, strong directional propagation and can be aggregated into a directionally narrow wire harness. It has strong reflection ability, high power, concentrated energy and is much larger than the general acoustic wave. It has diffraction, projection and other characteristics. The wire harness makes the bubble surface have a certain velocity gradient, which can destroy the adhesion of the particles and thus break away from the surface of the cleaned object. It is often used for cleaning workpieces with complex surface shapes, fine holes and slits. Ultrasonic cleaning can be used not only to clean medical devices but also for post-processing in additive manufacturing [117]. Changing the process parameters of ultrasonic cleaning can effectively remove the adhesive powder. For example, Tan [118] studied the influence of cavitation intensity on it, and proposed a high-strength ultrasonic cleaning process. It was found that by increasing the cavitation intensity of ultrasonic cleaning, some of the melted adhesive powder that is difficult to remove in additive manufacturing can be removed, which improves the cleaning efficiency and the cleanliness of additive manufacturing samples. In addition, ultrasonic cleaning can also clean the lattice structure. For example, Lyczkowska et al. [119] used ultrasonic cleaning to clean the lattice structure, which verified that ultrasonic cleaning can effectively remove loose and unmelted powder. Wang et al. [120] added ultrasonic cleaning in the post-processing cleaning process, and the removal rate of loose particles exceeded 90%.

**Table 1.** The advantages and disadvantages of ultrasonic cleaning.

| Advantages | Disadvantages |
|---|---|
| Low cost<br>Can be cleaned in batches<br>Comprehensive cleaning range<br>Wide applicability<br>Environmental safety | Very time consuming<br>May cause damage<br>There is noise |

### 3.2.2. Solid Medium Spray

The impact of high-speed solid medium flow is used to treat the surface of the sample and the interior of the pore structure to achieve the purpose of cleaning up the residual metal powder. More used are sandblasting [41,121] and dry ice spray [122]. The advantages and disadvantages are shown in Tables 2 and 3.

**Table 2.** The advantages and disadvantages of sandblasting.

| Advantages | Disadvantages |
|---|---|
| Simple operation<br>Thorough effect<br>Environmental pollution-free<br>High efficiency<br>Wide application range | High cost<br>Will introduce sand particles<br>Maintenance of machinery equipment |

**Table 3.** The advantages and disadvantages of dry ice jetting.

| Advantages | Disadvantages |
|---|---|
| Fast process speed<br>Low abrasiveness<br>No secondary waste generated | Operational difficulties<br>Raw materials difficult to store<br>There are security risks |

Sandblasting technology uses compressed air as the power to form a high-speed jet beam, and the abrasive is sprayed onto the sample to be processed at high speed. Due to the impact and cutting effect of the abrasive on the sample, the loose or adhered powder is peeled off from the sample so that the sample can obtain a certain degree of cleanliness and a different roughness, and improve the mechanical properties. The main parameters affecting the blasting effect are jet angle, compressed air pressure and abrasive clock. Abrasive is divided into metal abrasives and non-metallic abrasives. Common sandblasting abrasives include quartz sand, brown corundum, steel sand, etc. Initially, sandblasting was used as a post-treatment process for mechanical parts to clean up dirt and impurities on the formed surface of additive manufactured mechanical parts, and later was also specifically used to treat adhering powder. Adam and Zimmer's [123] research shows that sandblasting successfully removes residual powder from the channels of specimens produced by additive manufacturing with a diameter-to-length ratio of less than 1: 200. Moon et al. [124] successfully removed the adhering powder inside the sample by using compressed air to accelerate the injection of 120 particles the size of alumina particles by the blast nozzle. Their study found that when the jet angle is 60° and the compressed air pressure is 0.5 MPa, the effect of sandblasting to remove adhering powder is the best.

Dry ice jetting has been industrially tested since the 1980s and is the latest clean technology established in many industries, and there is growing interest in this technology [125]. The process is based on pneumatic injection and uses dry ice particles as a one-way injection medium. Dry ice particles are composed of solid carbon dioxide with a temperature of −78.5Â °C [126]. Hoenig et al. [127] proved that a cleaning system using soft matter flowing through the surface can be used to remove smaller particles. Carbon dioxide is the best soft material, and there is no secondary pollution after cleaning because dry ice will eventually sublimate under indoor conditions. Sherman et al. [128] found that dry ice injection is a gas–solid two-phase jet operation of gaseous carbon dioxide and dry ice particles, which has very good performance in removing particulate impurities. Toscano and Ahmadi [129] studied the mechanism of dry ice jetting to remove powder particles by introducing a torque balance model (rolling separation model) and force balance model (sliding separation model). Liu et al. [130] described the process of removing powder particles by impinging dry ice jet, quantitatively analyzed the particle removal efficiency and the influence of process parameters of dry ice injection on removal efficiency was discussed. The main parameters affecting the removal effect of dry ice jet are compressed air pressure, jet angle and dry ice mass. The research shows that the powder removal effect of dry ice jet is the best when the compressed air pressure is 0.4~1.2 Mpa, the dry ice mass is between 125 and 135 kg/h and the jet angle is between 60° and 90°.

#### 3.2.3. Chemical Cleaning

Chemical cleaning refers to the use of chemical reagents to treat the surface of the sample and the interior of the pore structure to achieve the purpose of cleaning the residual metal powder. Chemical cleaning is a promising process [131] for parts with complex set shapes; the advantages and disadvantages are shown in Table 4. For the sample of titanium alloy as raw material in medical additive manufacturing, HF or HNO3 mixture is mostly used for chemical cleaning. Surmeneva et al. [132] fabricated a porous Ti6Al4V titanium alloy bone scaffold by using EBM technology, found a large amount of powder adhesion and used HF/HNO3 to perform graded chemical etching on the sample. The results clearly show that the grading of etching time can promote the removal of powder particles attached to the surface and remove the powder inside the structure without seriously reducing the mechanical properties. Lyczkowska et al. [119] used a mixture of 80% $H_2O$, 6% HF and 14% HNO3, followed by a mixture of 99% $H_2O$ and 1% HF, to chemically polish SLM-printed bone scaffolds to improve surface quality and remove loose powder particles in porous structures. Brecht et al. [113] successfully removed residual powder particles in bone scaffolds produced by additive manufacturing using chemical etching agents based on HCl and $H_2O_2$.

**Table 4.** The advantages and disadvantages of chemical cleaning.

| Advantages | Disadvantages |
|---|---|
| Good cleaning effect<br>Efficient<br>Cost is lower | Will produce wastewater<br>Complex operation |

#### 3.2.4. Acoustic Dry Cleaning

The surface of the sample and the interior of the pore structure are treated by the oscillation effect of the acoustic wave to achieve the purpose of cleaning up the residual metal powder. The advantages and disadvantages are shown in Table 5. Buhl et al. [133] used high-intensity low-frequency sound to remove and collect residual powder. Gibbs et al. [134] found that the residual powder of metal materials can be cleaned by low-frequency acoustic waves. Seiffer et al. [135] explored the relationship between powder detachment rate and acoustic frequency when removing powder by acoustic waves. A frequency between 28 khz and 40 khz works best.

**Table 5.** The advantages and disadvantages of acoustic dry cleaning.

| Advantages | Disadvantages |
|---|---|
| Comprehensive cleaning<br>Pollution free<br>Simplicity of operation | Inefficiency<br>Expensive equipment |

In the early days, there were some methods to remove the residual powder, such as microwave boiling [136] and vacuum pumping. However, because the metal reflects the microwave, the microwave cannot be vibrated to the metal material, so it was gradually replaced by other technologies.

## 4. General Characterization Method

### *4.1. Optical Inspection Method*

The optical inspection method can determine the presence of residual insoluble particles in the porous structure of the repeated unit lattice under the premise that the unit lattice arrangement of the product structure allows full thickness light transmission. Firstly, the conventional open space of the unit is aligned with the light source and imaging equipment; the light source can be a lamp or fiber optic lamp. Secondly, the microscope focusing function is used to ensure clear visualization of the open space. Blocked or closed pores are shielded and may indicate that residual material is trapped within the lattice structure; finally, the visible area of the blocked pores can be measured to obtain semi-quantitative results, so as to confirm whether there are residual insoluble particles [137].

### *4.2. Microscopy*

Use one or more suitable equipment such as X-ray microscope (XRM), optical microscope or scanning electron microscope to observe the sample, clear photos are recorded and retained (with or without residual metal powder, residue particle count) with different magnifications ($n \geq 2$) that can explain the cleaning effect [137]. Thin porous structures (two apertures and less thickness) can be observed non-destructively. The residual insoluble particles can be directly observed by X-ray microscope (XRM), optical microscope or scanning electron microscope (Figure 7); the thicker porous structure can be embedded with a transparent embedding medium to realize the fixation of internal particles, cut by the standard metallographic analysis method and the residual particles can be quantified by metallographic microscope or SEM image. Inlay should be confirmed to ensure that loose insoluble particles of the inlay medium are not introduced during the cutting process. The inspection plane is cut out with a toothless saw or wire cutting along the specified position to observe whether the residual insoluble particles attached to the device. Schllephake et al. [138] studied the morphology of the released titanium particles; transmission electron microscopy was used to observe the ultrastructure and metal particles on the titanium plate for the treatment of jaw fractures. Hasib et al. [139] used abrasive cutting to divide the Ti-6Al-4V honeycomb structure into two parts parallel to the build direction. Next, the parting surface is polished to obtain the best surface for microscopic examination. The areas with and without powder in the mesh can be clearly distinguished by a digital microscope, and the amount of residual powder is measured by a surface area measurement.

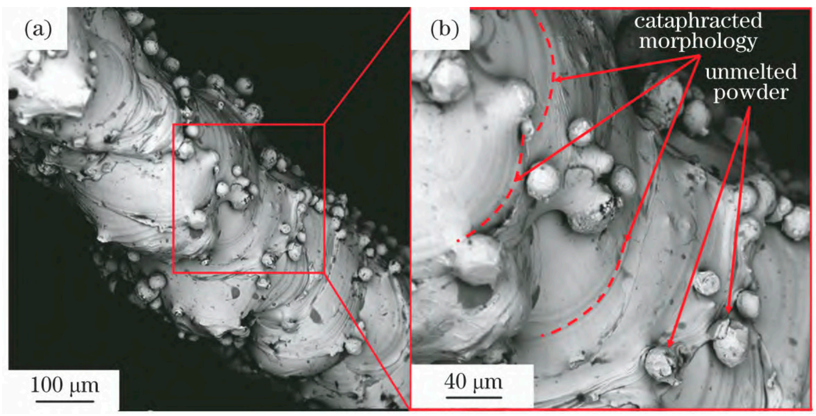


**Figure 7.** SEM images of microscopic profile.(**a**) Surface topography; (**b**) partially enlarged drawing. Reprinted with permission from Ref. [140]. Copyright2022, copyright Liu Y, Guo J, Shi W.

### 4.3. Micro-CT Examination

Micro-CT (micro computed tomography), is a non-destructive 3D imaging technique that allows a clear understanding of the internal microstructure of a sample without damaging it. Micro-CT can provide complete geometric and structural information. The former includes the size, volume and spatial coordinates of each point of the sample, and the latter includes material information such as attenuation value, density and porosity of the sample. In addition, the finite element analysis function of SCANCO can also provide mechanical parameters such as elastic modulus and Poisson's ratio of the tested material, and analyze the stress and strain of the sample. Therefore, the presence of residual insoluble particles in highly complex instruments can be assessed by micro-CT, which indirectly evaluates the residual amount of the powder in the open space of the part and the level of particle residue by calculation. James Robert [141] found that micro-CT is relatively mature in additive manufacturing. As a method to determine the porosity and geometry of printed samples, in some cases, the presence of inclusions or contaminants can also be determined. Hunter et al. [142] used micro-CT to observe powder adhesion inside porous structures formed by additive manufacturing.

### 4.4. Sample Weighing Method—Codification

After cleaning and verification, the sample was dried to constant weight and weighed with a balance with an accuracy of no less than 0.0001 g, denoted as $m_0$. After processing, the sample was dried to constant weight and weighed, denoted as $m_1$, and the mass change before and after processing was calculated as $\Delta m_1 = m_0 - m_1$, which is the residual amount of metal powder; after another cleaning, the sample was dried to constant weight, weighed, denoted as $m_2$, and the cleaning effect was characterized by $m_1 - m_2$.

### 4.5. Surface Roughness Measurement

The surface roughness is a microscopic geometric error that has an important influence on the service life and reliability of mechanical products. The roughness of the formed part was measured by surface roughness measuring instruments such as automatic stereo zoom microscope, and then the defect degree of the formed part was analyzed by combining the data of surface morphology and surface roughness [143,144]. Shi et al. [70] analyzed the influence of surface roughness by changing laser parameters, and found that process parameters affected the generation of surface defects. Defects are usually powder sticking, spheroidization and splashing, and these defects affect the flatness of the surface, which is also the main reason for the surface roughness. It was found that if the process parameters are not adjusted well, some of the powder will not melt in time, splash out from the molten pool, and then bond the unmelted powder to form sticky powder, resulting in significant surface defects and higher surface roughness [76]. The complex structure can be embedded with a transparent medium to realize the fixation of internal particles. The standard metallographic analysis method was used to cut, and the surface roughness was measured after cutting.

## 5. Application of Additive Manufacturing Titanium Alloy in Medical Field

The drugs produced by additive manufacturing generally do not use titanium alloys and use polycaprolactone (PCL) materials with the advantages of biodegradability, drug permeability and biocompatibility. Medical titanium alloys based on additive manufacturing are mainly used in orthopedic implants and medical devices. Orthopedic implants include artificial prostheses, bone joints, interbody fusion cages, bone plates, artificial bone trabeculae, etc. Medical devices include prostheses and orthopedic instruments, etc.

### 5.1. Orthopedic Implants

Titanium alloy is widely used in the production of orthopedic implants due to its good properties. Bone is mainly composed of outer cortical bone and inner cancellous bone, and the elastic modulus is about 0.5 GPa and 10–20 GPa [145]. The elastic modulus of dense titanium alloy is about 110 GPa. The elastic modulus of titanium alloy printed by additive manufacturing is lower than that of ordinary titanium alloy and is closer to the physiological structure of bone [146]. Titanium alloy has good biocompatibility, is conducive to bone ingrowth and osseointegration and is suitable for the preparation of orthopedic implants [147]. Titanium alloy not only has rigidity, but also has outstanding flexibility and good fatigue resistance. It is suitable as a joint support and can replace other metal materials. Titanium alloy is insoluble in strong acid and alkali and has high specific strength at 500 °C. It is non-toxic to the human body and has good chemical stability, which is suitable for implantation in the human body [148]. Titanium alloy has good corrosion resistance, fatigue resistance and stability. Compared with other metal materials, its elastic modulus is closer to bone and is suitable for orthopedic applications.

It is estimated that more than 2 million bone transplants, 280,000 hip fractures, 700,000 spinal fractures, 250,000 wrist fractures and 700,000 skull repairs are performed worldwide each year [149]. Due to the complex shape of human bones, bone defect reconstruction is one of the most difficult challenges faced by surgeons. With the increase in traffic accidents and tumors, bone defects increase sharply, thus increasing the demand for orthopedic implants. In these cases, some experts have proposed medical titanium alloy custom orthopedic implants based on additive manufacturing.

#### 5.1.1. Skull Implants

There are situations where implants are not subjected to significant and rather continuous bearing or other stresses, and can serve as bone replacement. This is especially true for skull-bone-related implants, as illustrated in Figure 8. Murr reported a reticular skull implant made by EBM technology [150]. Wadea Ameen et al. [151] successfully manufactured thin titanium alloy skull implants for skull defect reconstruction by using EBM technology; the porosity is 49.81% and the pore size is 700 μm. Alida Mazzoli et al. [152] realized the cooperation of CT imaging, computer modeling and additive manufacturing technology, and formed a titanium alloy skull implant with biocompatibility by additive manufacturing. Zhao et al. [153] found that personalized titanium alloy skull prostheses based on additive manufacturing printing have better impact resistance, but also can effectively repair skull defects and protect intracranial brain tissue.

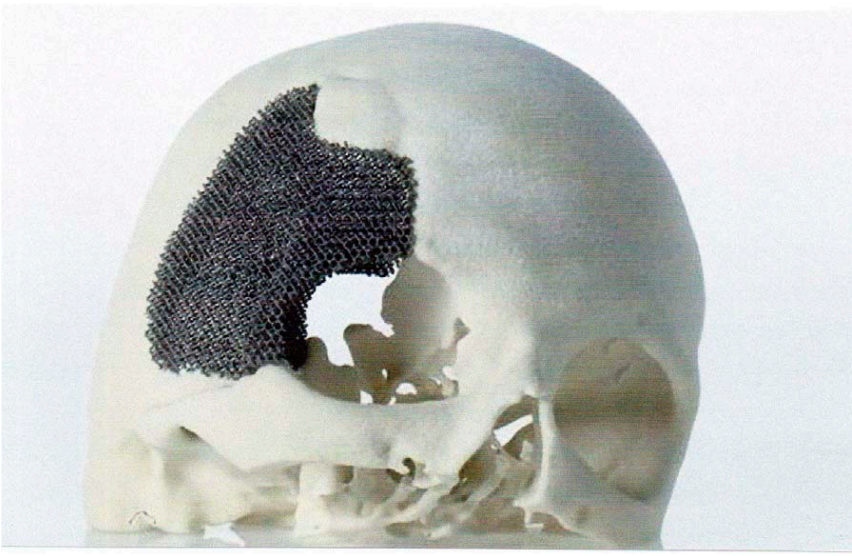

**Figure 8.** Rhombic dodecahedral element reticulated Ti-6Al-4V mesh skull replacement prototype fabricated by EBM. Reprinted with permission from Ref. [150]. Copyright 2017, copyright Murr L E.

#### 5.1.2. Jaw Implants

Tian Kaiyue et al. [154] used porous scaffolds of titanium alloy made by laser selective melting technology to repair jaw defects. The study found that jaw implants made of titanium alloy based on additive manufacturing were feasible as substitute materials for bone defects. Yan et al. [155] used Ti-6Al-4V titanium alloy to fabricate a mandibular prosthesis with a 3D mesh porosity of 81.38% and a strut size of 0.7 mm by EBM, which meets the requirements for implantation in a human body (Figure 9). Moiduddin et al. [156] used Ti-6Al-4V titanium alloy powder to obtain titanium cheekbone implants by EBM technology and verified its feasibility. Mommaerts [157] fabricated titanium periosteal mandibular implants using additive manufacturing technology, which provides another solution for patients with extreme jaw atrophy. At the same time, the International Working Group on Additive Manufacturing of Mandibular Implants conducted multiple studies. After one year, 15 patients with permanent mandibular implants were followed up. All patients had normal lives and no complications. It is proved that additive manufacturing is a promising tool for patients with extreme jaw atrophy and meets the high expectations of patients without complications [158].

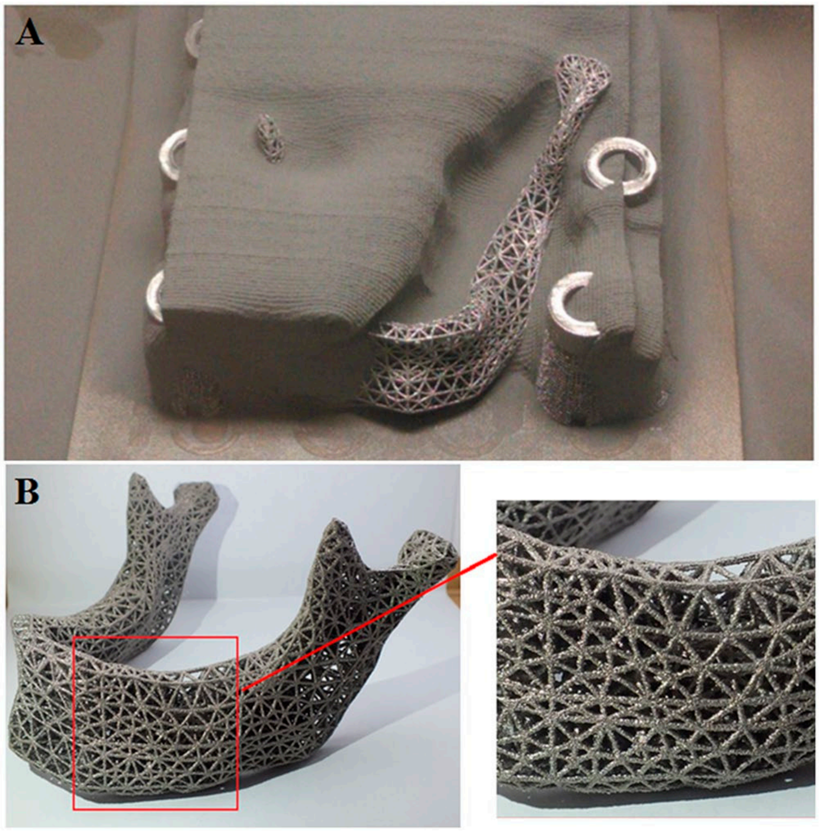


**Figure 9.** Preparation of Ti6Al4V scaffolds by EBM. (**A**) The parts are cleaned up to remove loose titanium powder lodged within the 3D mesh structure. (**B**) 3D mesh titanium mandibular prosthesis scaffold fabricate using EBM technology. Reprinted with permission from Ref. [155]. Copyright 2018, copyright Yan R, Luo D, Huang H.

#### 5.1.3. Dental Implant

Tooth defect or tooth loss seriously affects people's health. With the acceleration of population aging, the number of edentulous patients in China has reached 15 million, and the number of patients with tooth defects has exceeded 300 million [159]. It is an urgent task to provide comfortable and safe denture restoration methods with high chewing efficiency. With the development of the social economy and the progression of science and technology, people's requirements for quality of life continue to improve, and the preparation of personalized dental implants has become the first choice for oral rehabilitation. As a routine procedure for replacing missing teeth, implanted dentures demonstrated significant oral functional rehabilitation and excellent long-term prognosis [160]. Wang et al. [161] used

MTT colorimetric experiments to verify that the titanium alloy dental implant printed by additive manufacturing technology has a cytotoxicity level that meets the clinical application requirements of oral implant materials. The titanium dental implant formed by Tolochko et al. [162] using additive manufacturing technology meets the requirements of medical dental implants. Koike et al. [163] compared the fatigue life of different titanium alloy dental implants based on additive manufacturing. Gonzalez and Rosca [164] proved the passivation and corrosion resistance of titanium alloy dental implants by additive manufacturing. New Zealand rabbits are widely used to evaluate the function of dental implants. Therefore, Hamza et al. carried out animal experiments with titanium alloy dental implants formed by SLM. The results showed that the dental implants formed by titanium alloy powder did not cause rejection in animals, and the osseointegration effect was the best [165]. Zhou et al. [166] fabricated titanium alloy dental implants as shown in Figure 10 by SLM technology.

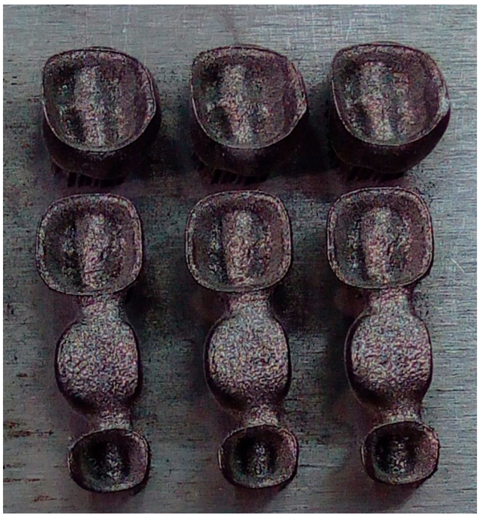

**Figure 10.** Crown and dental bridge printed via SLM with titanium alloy. Reprinted with permission from Ref. [166]. Copyright 2017, copyright Zhou H, Fan Q.

5.1.4. Spinal Implants

Scholars believe that through the use of AM, it is possible to manufacture porous titanium cages with better loadbearing characteristics, less micromotion, high compressive strength, osteoconductivity and bone-bonding ability, eliminating the need for autografting, and possessing interconnected pores for easy fluid flow [167,168]. China's Huaxiang Group's spinal implants of titanium alloy with lattice shapes, printed by selective laser melting, have been recognized by the National Medical Products Administration (NMPA). In 2017, the US Food and Drug Administration (FDA) approved two additive manufacturing titanium alloy spinal implants. One is a 3D-printed titanium vertebral body implant HAWKEYE Ti and the other is a NEXXT MATRIXX 3D-printed spinal implant. Hollander et al. [169] fabricated porous spinal implants with different pore sizes using additive manufacturing technology and verified that the surface of the implant allowed the growth of human osteoblasts. Lin et al. [170] obtained a porosity of 55% using SLM, exhibiting a compressive elastic modulus comparable to that of natural bone (2.97 GPa) and achieving higher bone growth efficiency compared with a traditional PEEK cage. A case of C2 spondylectomy and reconstruction was recorded by Xu et al. A 12-year-old boy with Ewing's sarcoma was implanted with an AM vertebral implant. Xu et al. fabricated vertebral implants with Ti-6Al-4V titanium alloy [171]. Shunsuke et al. [172] verified the effectiveness and safety of the porous active titanium spinal fusion device fabricated by additive manufacturing (Figure 11).

**Figure 11.** Photograph of porous bioactive titanium device for transforaminal lumbar interbody fusion. Reprinted with permission from Ref. [172]. Copyright 2011, copyright Fujibayashi S, Takemoto M, Neo M, Matsushita T, Kokubo T, Doi K, Ito T, Shimizu A, Nakamura T.

#### 5.1.5. Chest Implants

In 2013, Turna et al. reported the first 3D-printed chest implant. It consisted of a plate for the sternum and ribs [173]. Alvarez et al. [174] fabricated titanium alloy chest implants using additive manufacturing technology to reconstruct large chest wall resection and maintain thoracic integrity. Additionally, the implant provided excellent aesthetic and functional effects. The virtual planning and production of preoperative implants reduces the operation time and uncertainty, and improves the safety and accuracy. Six months after implantation, there were no complications such as pain, infection, dislocation or abnormal movement related to implantation. Goldsmith et al. [175] reconstructed bone defects in patients with titanium alloy ribs and hemisternal implants by using powder bed fusion technology. The patient was also reviewed 18 months after the procedure and was found to have no symptoms and did not describe pain, local tenderness or dyspnea. Goldsmith et al. made the titanium alloy chest implant shown in Figure 12. Liu et al. [176] used titanium alloy artificial ribs made by additive manufacturing to apply to patients with partial resection of ribs and sternoclavicular bones. As a result, four operations were successful and no surgical complications occurred.

**Figure 12.** Three-dimensional printed titanium alloy chest implants. Reprinted with permission from Ref. [175] Copyright 2020, copyright Goldsmith I, Evans P, Goodrum H, Warbrick-Smith J, Bragg T.

#### 5.1.6. Pelvic Implants

In trauma patients, pelvic injury is not uncommon, mainly due to impact, rolling, extrusion, high fall and other damage. In the past, additive manufacturing technology was mainly used to assist in preoperative diagnosis and simulated surgery of pelvic fractures. Later, more and more studies have proved the feasibility of additive manufacturing of titanium alloy pelvic implants [177,178]. Wong et al. [179] used titanium alloy to manufacture pelvic special implants and then implanted them and verified the effect. Broekhuis et al. [180] customized and designed titanium alloy pelvic implants for acetabular reconstruction after tumor resection using additive manufacturing technology. Park et al. [181] used EBM technology to make a pelvic implant with less pore defects (Figure 13), which was successfully applied to a 35-year-old woman with Ewing's sarcoma of the left pelvis. In order to enhance the inward growth of the bone, the connection between the bone and the implant was designed as a lattice structure.


**Figure 13.** Pelvic implant manufactured by metal 3D printing for a 35-year-old woman who received surgery for Ewing sarcoma of the left pelvis. (**a**) Designs and (**b**) photographs revealed that the pelvic implant has both solid and lattice structures. (**c**) A postoperative plain radiograph of the applied pelvic implant. Reprinted with permission from Ref. [181]. Copyright 2022, copyright Park J, Park H, Kim J, Kim H, Yoo C, Kang H.

In addition to the above major organ implants, there are also titanium alloy bone scaffolds (Figure 14) [182], bone plates [183], hollow screws [184], hip joints [185], knee joints [186], etc.

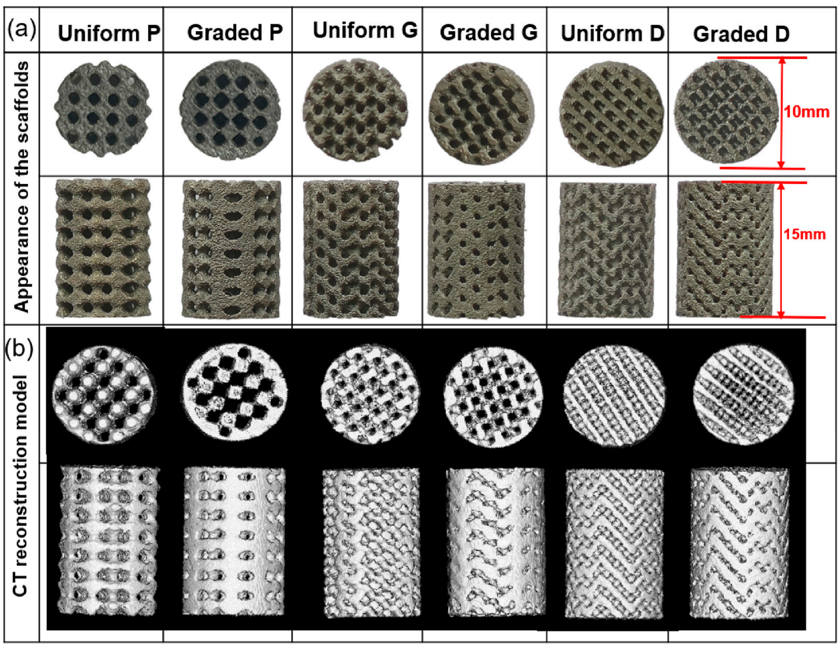


**Figure 14.** Titanium alloy bone scaffold. (**a**) Macroscopic feature image of the scaffolds, (**b**) scaffolds model image obtained by micro-CT. Reprinted with permission from Ref. [182]. Copyright 2022, copyright Lv Y, Wang B, Liu G.

### 5.2. Medical Devices

Medical devices are mainly concentrated in prostheses and orthopedic instruments. Loss of a limb is a traumatic event; whether as a result of an accident, a fight or a decision to tackle a growing tumor or other worsening disease, amputation can have a lasting impact on a patient's quality of life and can cause distress to the patient's family and friends. Therefore, it is necessary to have a prosthetic leg or arm that can meet the mechanical requirements for a long time, so that the patient can fully restore motor functions such as standing and walking. However, the use of modern additive manufacturing technology can improve artificial arms and legs. Based on these technologies, low-cost and fully functional prostheses can be produced for amputees. For example, Herbert et al. [187] used an efficient, simple additive manufacturing technology to develop a simple titanium alloy prosthetic foot that can be used comfortably by patients. Zuniga et al. [188] prepared a low-cost 3D-printed hand for children with upper limb dislocation. The results of the subsequent survey showed that prosthetic hands can have a positive impact on the quality of life of children in a variety of activities at home and school. The ability of foot orthoses [189], ankle–foot orthoses [190] and wrist splints customized by additive manufacturing technology has been proved to have good adaptability and sufficient strength in limited clinical evaluation.

## 6. Summary and Outlook

In this paper, the phenomenon and causes of powder adhesion are reviewed from the perspective of the process involved in additive manufacturing. The influence of different processes on the powder adhesion of titanium alloy forming parts is expounded. The mainstream powder adhesion removal methods are introduced, and the application of additive manufacturing titanium alloy in the medical field is reviewed. In summary, compared with traditional manufacturing technology, additive manufacturing has unparalleled advantages. With the rapid development of society and the improvement of people's living standards in recent years, people pay more and more attention to their own health and have higher requirements for quality of life. Therefore, medical devices customized according to individuals have become a trend, which has promoted the application of additive manufacturing technology in the medical field. More and more extensively, the use of titanium alloy as raw material for additive manufacturing technology has especially become a research hotspot. The application prospect of titanium alloy additive manufacturing technology in the medical field is very broad.

However, in the medical field, the key problem restricting the application of titanium alloy additive manufacturing technology is still the problem of adhesion powder. The domestic and foreign scholars for titanium alloy additive manufacturing technology research mostly focused on mechanical properties and biological properties, etc. The removal and characterization of internal adhering powder is a relatively small degree of research. Therefore, it is necessary to develop new and better medical titanium alloy additive manufacturing internal and surface powder removal technology that is suitable for the complex structure of titanium alloy and forms a perfect, nondestructive and testing-efficient cleaning method.

**Author Contributions:** X.Z.: conceptualization, resources, investigation, methodology, formal analysis, writing—original draft, writing—review and editing. Y.L.: validation, writing—original draft, writing—review and editing. S.L.: conceptualization, investigation, validation, visualization, writing—original draft, resources. H.G.: conceptualization, investigation, validation, visualization, writing—original draft, resources. W.S.: formal analysis, investigation, resources, visualization, writing—original draft, writing—review and editing. All authors have read and agreed to the published version of the manuscript.

**Funding:** This research was funded by National Natural Science Foundation of China grant number 51975006, 51505006. This research was funded by National Key Research and Development Program of China grant number 2022YFC2406004. This research was funded by The Research Foundation for Youth Scholars of Beijing Technology and Business University grant number 19008022158.

**Data Availability Statement:** The raw/processed data required to reproduce these findings cannot be shared at this time as the data also form part of an ongoing study.

**Conflicts of Interest:** The authors declare that they have no conflict of interest.

## References

1. Bandyopadhyay, A.; Zhang, Y.; Bose, S. Recent Developments in Metal Additive Manufacturing. *Curr. Opin. Chem. Eng.* **2020**, *28*, 96–104. [CrossRef] [PubMed]
2. Zeng, S. Research progress of metal additive manufacturing technology. *China Metal Bulletin.* **2022**, *4*, 186–188.
3. Xiong, J.; Yang, J.; Zhang, J.; Guo, J. Research progress of metal additive manufacturing. *China Mater. Technol.* **2021**, *30*, 107.
4. Dong, C.; Tan, J.; Lin, Z.; Wang, C.; Zhao, Y. Research progress on additive manufacturing technology of titanium alloy. *Met. Process. (Hot Process.)* **2020**, *07*, 16–21.
5. Dang, X.; Wang, J. Research Status and Prospect of Additive Manufacturing Technology at Home and Abroad. *Aviat. Precis. Manuf. Technol.* **2020**, *56*, 35–38.
6. Kermavnar, T.; Shannon, A.; O'Sullivan, L. The application of additive manufacturing/3D printing in ergonomic aspects of product design: A systematic review. *Appl. Ergon.* **2021**, *97*, 103528. [CrossRef]
7. Mohanavel, V.; Ashraff, K.; Ranganathan, S.; Allen, J.; Ravikumar, M.; Rajkumar, S. The roles and applications of additive manufacturing in the aerospace and automobile sector. *Mater. Today Proc.* **2021**, *47*, 405–409. [CrossRef]
8. Schutz, R.; Watkins, H. Recent developments in titanium alloy application in the energy industry. *Mater. Sci. Eng. A* **1998**, *243*, 305–315. [CrossRef]
9. Zhang, Z.; Liu, S.; Yang, X.; Wang, Y.; Shi, M.; Zhang, G. Application and Prospect of Additive Manufacturing in Porous Metal Implants. *Therm. Process.* **2019**, *48*, 1–5.
10. Attarilar, S.; Salehi, M.T.; Fadhalah, K. Functionally Graded Titanium Implants: Characteristic Enhancement Induced by Combined Severe Plastic Deformation. *PLoS ONE* **2019**, *14*, e0221491. [CrossRef]
11. Spataru, M.-C.; Cojocaru, F.D.; Sandu, A.V.; Solcan, C.; Duceac, I.A.; Baltatu, M.S.; Voiculescu, I.; Geanta, V.; Vizureanu, P. Assessment of the Effects of Si Addition to a New TiMoZrTa System. *Materials* **2021**, *14*, 7610. [CrossRef]
12. Bălţatu, M.S.; Vizureanu, P.; Geantă, V.; Nejneru, C.; Ţugui, C.A.; Focşăneanu, S.C. Obtaining and Mechanical Properties of Ti-Mo-Zr-Ta Alloys. *IOP Conf. Ser. Mater. Sci. Eng.* **2017**, *209*, 012019. [CrossRef]
13. Roach, P.; Eglin, D.; Rohde, K. Modern Biomaterials:A Review Bulk Properties and Implications of Surface Modifications. *J. Mater. Sci. Mater. Med.* **2007**, *18*, 1263–1277. [CrossRef]
14. Triyono, J.; Alfiansyah, R.; Sukanto, H. Fabrication and Characterization of Porous Bone Scaffold of Bovine Hydroxyapatite-glycerin by 3D Printing Technology. *Bioprinting* **2020**, *18*, e00078. [CrossRef]
15. Parthasarathy, L.; Starly, B.; Raman, S.; Christensen, A. Mechanical evaluation of porous titanium (Ti6Al4V) structures with electron beam melting (EBM). *J. Mech. Behav. Biomed. Mater.* **2010**, *3*, 249–259. [CrossRef]
16. Basalah, A.; Esmaeili, S.; Toyserkani, E. On the influence of sintering protocols and layer thickness on the physical and mechanical properties of additive manufactured titanium porous bio-structures. *Mater. Process. Technol.* **2016**, *238*, 341–351. [CrossRef]
17. Bansiddhi, A.; Dunand, D. 7—Titanium and NiTi foams for bone replacement. In *Bone Substitute Biomaterials*; Woodhead Publishing: Cambridge, UK, 2014; pp. 142–179.
18. Nouri, A. 5—Titanium foam scaffolds for dental applications. In *Metallic Foam Bone*; Woodhead Publishing: Cambridge, UK, 2017; pp. 131–160.
19. Kokubo, T.; Yamaguchi, S. Novel bioactive materials developed by simulated body fluid evaluation: Surface-modified Ti metal and its alloys. *Acta Biomater.* **2016**, *44*, 16–30. [CrossRef]
20. Xu, W.; Brandt, W.; Sun, S.; Elambasseril, J.; Liu, Q.; Latham, K. Additive manufacturing of strong and ductile Ti–6Al–4V by selective laser melting via in situ martensite decomposition. *Acta Mater.* **2015**, *85*, 74–84. [CrossRef]
21. Rani, V.D.; Vinoth-Kumar, L.; Anitha, V.; Manzoor, K.; Deepthy, K.; Shantikumar, V. Osteointegration of titanium implant is sensitive to specific nanostructure morphology. *Acta Biomater.* **2012**, *8*, 1976–1989. [CrossRef]
22. Biesiekierski, A.; Wang, J.; Gepreel, M.; Wen, C. A new look at biomedical Ti-based shape memory alloys. *Acta Biomater.* **2012**, *8*, 1661–1669. [CrossRef] [PubMed]
23. Balaji, V.; Kumaran, S. Densification and microstructural studies of titanium-boron carbide (B4C) powder mixture during spark plasma sintering. *Powder Technol.* **2014**, *264*, 536–540. [CrossRef]
24. Chen, G.; Li, N.; Fu, X.; Zhou, W. Preparation and characterization of a sodium polyacrylate/sodium silicate binder used in oxidation resistant coating for titanium alloy at high temperature. *Powder Technol.* **2012**, *230*, 134–138. [CrossRef]
25. Manshadi, A.; Bermingham, M.; Dargusch, M.; StJohn, D.; Qian, M. Metal injection moulding of titanium and titanium alloys: Challenges and recent development. *Powder Technol.* **2017**, *319*, 289–301. [CrossRef]
26. Hong, S.; Park, J.; Park, K.; Kim, K.; Lee, J.; Lee, K. Fabrication of titanium carbide nano-powders by a very high speed planetary ball milling with a help of process control agents. *Powder Technol.* **2015**, *274*, 393–401. [CrossRef]
27. Huang, B.; Fan, C.; Pan, C.; Zheng, A.; Ma, X.; Li, Y. Synthesis and catalytic oxidation property of titanium-zirconium mixed oxide microsphere as well as titanium oxide microcube. *Powder Technol.* **2017**, *315*, 258–269. [CrossRef]

28. Klisiewicz, P.; Roberts, J.; Pohlman, N. Segregation of titanium powder with polydisperse size distribution: Spectral and correlation analyses. *Powder Technol.* **2015**, *272*, 204–210. [CrossRef]
29. Kumaran, S.; Sasikumar, T.; Arockiakumar, R.; Srinivasa, T. Nanostructured titanium aluminides prepared by mechanical alloying and subsequent thermal treatment. *Powder Technol.* **2008**, *185*, 124–130. [CrossRef]
30. Kwon, H.; Kim, J.; Jung, S.; Suh, C.; Kil, D.; Roh, K. Premixed TiC–Ni composite powder prepared by mechanical milling of Ti–Ni alloy/graphite mixture and subsequent heat treatment. *Powder Technol.* **2014**, *253*, 681–685. [CrossRef]
31. Manonukul, A.; Tange, M.; Srikudvien, P.; Denmud, N.; Wattanapornphan, P. Rheological properties of commercially pure titanium slurry for metallic foam production using replica impregnation method. *Powder Technol.* **2014**, *266*, 129–134. [CrossRef]
32. Thavanayagam, G.; Pickering, K.; Swan, J.; Cao, P. Analysis of rheological behaviour of titanium feedstocks formulated with a water-soluble binder system for powder injection moulding. *Powder Technol.* **2015**, *269*, 227–232. [CrossRef]
33. Vivek, A.; DeFouw, J.; Daehn, G. Dynamic compaction of titanium powder by vaporizing foil actuator assisted shearing. *Powder Technol.* **2014**, *254*, 181–186. [CrossRef]
34. Yan, Z.; Chen, F.; Cai, Y. High-velocity compaction of titanium powder and process characterization. *Powder Technol.* **2011**, *208*, 596–599. [CrossRef]
35. Yan, Z.; Chen, F.; Cai, F.; Zheng, Y. Microstructure and mechanical properties of insitu synthesized TiB whiskers reinforced titanium matrix composites by highvelocity compaction. *Powder Technol.* **2014**, *267*, 309–314. [CrossRef]
36. Balazic, M.; Kopac, J.; Jackson, M. Titanium and titanium alloy applications in medicine. *Int. J. Nano Biomater.* **2007**, *1*, 3–34. [CrossRef]
37. Rack, H.; Qazi, J. Titanium alloys for biomedical applications. *Mater. Sci. Eng. C* **2006**, *264*, 1269–1277. [CrossRef]
38. Jackson, M.; Kopac, J.; Balazic, M. Titanium and titanium alloy applications in medicine. *Surg. Tools Med. Devices* **2016**, *1*, 475–517.
39. Kulkarni, M.; Mazare, A.; Schmuki, P. Biomaterial surface modification of titanium and titanium alloys for medical applications. *Nanomedicine* **2014**, *111*, 111.
40. Suard, M.; Martin, G.; Lhuissier, P. Mechanical equivalent diameter of single struts for the stiffness prediction of lattice structures produced by Electron Beam Melting. *Addit. Manuf.* **2015**, *8*, 124–131. [CrossRef]
41. Drescher, P.; Reimann, T.; Seitz, H. Investigation of powder removal of net–structured titanium parts made from electron beam melting. *Int. J. Rapid Manuf.* **2014**, *4*, 81–89. [CrossRef]
42. Harun, W.; Kamariah, M.; Muhamad, N. A review of powder additive manufacturing processes for metallic biomaterials. *Powder Technol.* **2018**, *327*, 128–151. [CrossRef]
43. Shi, W.; Yan, T.; Liu, Y. Simulation Analysis and Experimental Study on SLM Forming Titanium Alloy Milling Hole. *Metals* **2022**, *12*, 1919. [CrossRef]
44. Drescher, P.; Sarhan, M.; Seitz, H. An investigation of sintering parameters on titanium powder for electron beam melting processing optimization. *Materials* **2016**, *9*, 974. [CrossRef] [PubMed]
45. Jahadakbar, A.; Nematollahi, M.; Safaei, K. Design, modeling, additive manufacturing, and polishing of stiffness-modulated porous nitinol bone fixation plates followed by thermomechanical and composition analysis. *Metals* **2020**, *10*, 151. [CrossRef]
46. Cui, X.; Zhang, S.; Zhang, C.; Wu, C.; Wang, Q.; Dong, S. Research status and prospect of laser additive manufacturing of high performance functionally gradient materials. *Mater. Eng.* **2020**, *48*, 13–23.
47. Shi, Y. Industrial Application and Industrialization Development of 3D Printing Technology. *Mech. Des. Manuf. Eng.* **2016**, *45*, 11–16.
48. Cai, Y.; Han, H.; Ren, D.; Ji, H.; Lei, J. Effect of chemical etching process on surface roughness of TC4 titanium alloy formed by selective laser melting. *J. Mater. Res.* **2022**, *36*, 435–442.
49. *ASTM F2792-12a*; Standard Terminology for Additive Manufacturing Technologies Withdrawn 2015. ASTM International: West Conshohocken, PA, USA, 2012.
50. *GB/T 35021-201*; Standard Terminology for Additive Manufacturing Technologies China. Standards Press of China: Beijing, China, 2018.
51. Shaheen, M.; Thornton, A.; Luding, S. The influence of material and process parameters on powder spreading in additive manufacturing. *Powder Technol.* **2021**, *383*, 564–583. [CrossRef]
52. Oliveira, J.; LaLonde, P.; Ma, J. Processing parameters in laser powder bed fusion metal additive manufacturing. *Mater. Des.* **2020**, *193*, 108762. [CrossRef]
53. Ingrassia, T.; Nigrelli, V.; Ricotta, V. Process Parameters Influence in Additive Manufacturing. In *Advances on Mechanics, Design Engineering and Manufacturing*; Springer: Cham, Switzerland, 2017; pp. 261–270.
54. Mostafaei, A.; Elliott, A.; Barnes, J. Binder Jet 3D Printing: Process Parameters, Materials, Properties, Modeling, and Challenges. *Prog. Mater. Sci.* **2021**, *119*, 100707. [CrossRef]
55. Mostafaei, A.; Stevens, E.; Ference, J. Binder Jetting of a Complex-Shaped Metal Partial Denture Framework. *Addit. Manuf.* **2018**, *21*, 63–68. [CrossRef]
56. Gonzalez, J.; Mireles, J.; Lin, Y. Characterization of Ceramic Components Fabricated Using Binder Jetting Additive Manufacturing Technology. *Ceram. Int.* **2016**, *42*, 10559–10564. [CrossRef]
57. Wei, Q.; Heng, Y.; Mao, Y.; Feng, H.; Cai, C.; Cai, D.; Li, W. The development and prospect of metal binder spray additive manufacturing technology. *Packag. Eng.* **2021**, *42*, 103–119.

58. Li, M.; Du, W.; Elwany, A.; Pei, Z.; Ma, C. Metal Binder Jetting Additive Manufacturing: A Literature Review. *J. Manuf. Sci. Eng.* **2020**, *142*, 090801. [CrossRef]
59. Mostafaei, A.; Vecchis, P.; Nettleship, I. Effect of Powder Size Distribution on Densification and Microstructural Evolution of Binder-Jet 3d-Printed Al- loy 625. *Mater. Des.* **2019**, *162*, 375–383. [CrossRef]
60. Stevens, E.; Schloder, S.; Bono, E. Density variation in binder jetting 3D-printed and sintered Ti-6Al-4V. *Addit. Manuf.* **2018**, *22*, 746–752. [CrossRef]
61. Cox, S.; Thornby, J.; Gibbons, G. 3D Printing of Porous Hydroxyapatite Scaffolds Intended for Use in Bone Tissue Engineering Applications. *Mater. Sci. Eng. C* **2015**, *47*, 237–247. [CrossRef]
62. Jurisch, M.; Studnitzky, T.; Andersen, O. 3D screen printing for the fabrication of small intricate Ti-6Al-4V parts. *Powder Metall.* **2015**, *58*, 339–343. [CrossRef]
63. Chen, H.; Zhao, Y. Process parameters optimization for improving surface quality and manufacturing accuracy of binder jetting additive manufacturing process. *Rapid Prototyp. J.* **2016**, *22*, 527–538. [CrossRef]
64. Turker, M.; Godlinski, D.; Petzoldt, F. Effect of Production Parameters on the Properties of Ni 718 Superalloy by Three-Dimensional Printing. *Mater. Charact.* **2008**, *59*, 1728–1735. [CrossRef]
65. Parteli, E.; Pöschel, T. Particle-Based Simulation of Powder Application in Additive Manufacturing. *Powder Technol.* **2016**, *288*, 96–102. [CrossRef]
66. Gu, B. Application and development trend of additive manufacturing technology at home and abroad. *Met. Process. (Hot Process.)* **2022**, *3*, 1–16.
67. Zhang, H.; Yang, K. A review of current status and applications of additive manufacturing. *Packag. Eng.* **2021**, *42*, 9–15.
68. Zheng, Y.; Xia, D.; Chen, Y.; Liu, Y.; Xu, Y.; Wen, P.; Tian, Y.; Lai, Y. Additive manufacturing of degradable metal medical implants. *Met. J.* **2021**, *57*, 1499–1520.
69. Ma, C.; Zhao, Y. Research on the development strategy of denture customization and visualization collaborative service platform based on 3D printing. *China Equip. Eng.* **2021**, *22*, 128–129.
70. Shi, W.; Li, J.; Liu, Y. Experimental study on mechanism of influence of laser energy density on surface quality of Ti-6Al-4V alloy in selective laser melting. *J. Cent. South Univ.* **2022**, *29*, 3447–3462. [CrossRef]
71. Zhao, C.; Li, W.; Wang, Q.; Wang, Y.; Zhao, Y.; Di, S.; Ren, D.; Ji, B. Study on Internal Defects and Their Evolution of Titanium Alloy Formed by Selective Laser Melting. *Rare Met. Mater. Eng.* **2021**, *50*, 2841–2849.
72. Hou, G.; Wu, T.; Shang, Z.; Shao, Z. Application of digital surgery and additive manufacturing technology in reconstruction of mandibular defects with vascularized iliac bone flap. *Chin. J. Exp. Surg.* **2020**, *37*, 635–638.
73. Majumdar, T.; Eisenstein, N.; Frith, J.E.; Cox, S.C.; Birbilis, N. Additive Manufacturing of Titanium Alloys for Orthopedic Applications: A Materials Science Viewpoint. *Adv. Eng. Mater.* **2018**, *20*, 28. [CrossRef]
74. Sing, S.L.; An, J.; Yeong, W.Y.; Wiria, F.E. Laser and electron-beam powder-bed additive manufacturing of metallic implants: A review on processes, materials and designs. *J. Orthop. Res. Off. Publ. Orthop. Res. Soc.* **2016**, *34*, 369–385. [CrossRef]
75. Guo, J.; Xu, J.; Liu, B.; Fu, B.; Li, F. Research progress on the performance of 3D printed orthopedic titanium alloy medical devices. *China Pharm.* **2021**, *35*, 471–478.
76. Shi, W.; Han, Y.; Liu, Y.; Jing, Y. Selected area laser melting TC4 spheroidization splash mechanism and experimental research. *Surf. Technol.* **2021**, *50*, 75–82.
77. Le, T.; Lo, Y. Effects of sulfur concentration and Marangoni convection on melt-pool formation in transition mode of selective laser melting process. *Mater. Des.* **2019**, *179*, 107866. [CrossRef]
78. Yusuf, S.; Gao, N. Influence of energy density on metallurgy and properties in metal additive manufacturing. *Mater. Sci. Technol.* **2017**, *33*, 1269–1289. [CrossRef]
79. Ferro, P.; Meneghello, R.; Savio, G. A modified volumetric energy density–based approach for porosity assessment in additive manufacturing process design. *Int. J. Adv. Manuf. Technol.* **2020**, *110*, 1911–1921. [CrossRef]
80. Kluczyński, J.; Śnieżek, L.; Grzelak, K. The influence of exposure energy density on porosity and microhardness of the SLM additive manufactured elements. *Materials* **2018**, *11*, 2304. [CrossRef]
81. Körner, C. Additive Manufacturing of Metallic Components by Selective Electron Beam Melting—A Review. *Int. Mater. Rev.* **2016**, *61*, 361–377. [CrossRef]
82. Le, K.; Wong, C.; Chua, K. Discontinuity of overhanging melt track in selective laser melting process. *Int. J. Heat Mass Transf.* **2020**, *162*, 120284. [CrossRef]
83. Borgman, J.M.; Wang, J.; Zani, L.; Conway, P.P.; Torres-Sanchez, C. The Effect of Energy Density and Nb Content on the Microstructure and Mechanical Properties of Selective Laser Melted Ti-(10–30 Wt.%) Nb. *J. Mater. Eng. Perform.* **2021**, *30*, 8771–8783. [CrossRef]
84. Ge, J.; Yuan, B.; Zhao, L.; Yan, M.; Chen, W.; Zhang, L. Effect of Volume Energy Density on Selective Laser Melting Niti Shape Memory Alloys: Microstructural Evolution, Mechanical and Functional Properties. *J. Mater. Res. Technol.* **2022**, *20*, 2872–2888. [CrossRef]
85. Gibson, I.; Rosen, D.; Stucker, B. Directed energy deposition processes. In *Additive Manufacturing Technologies*; Springer: New York, NY, USA, 2015; pp. 245–268.
86. Ahn, D. Directed energy deposition (DED) process: State of the art. *Int. J. Precis. Eng. Manuf.-Green Technol.* **2021**, *8*, 703–742. [CrossRef]

87. Oh, W.; Lee, W.; Kim, M. Repairing additive-manufactured 316L stainless steel using direct energy deposition. *Opt. Laser Technol.* **2019**, *117*, 6–17. [CrossRef]
88. Fujishima, M.; Oda, Y.; Ashida, R. Study on factors for pores and cladding shape in the deposition processes of Inconel 625 by the directed energy deposition (DED) method. *CIRP J. Manuf. Sci. Technol.* **2017**, *19*, 200–204. [CrossRef]
89. Shalnova, S.; Kuzminova, Y.; Evlashin, S. Effect of recycled powder content on the structure and mechanical properties of Ti-6Al-4V alloy produced by direct energy deposition. *J. Alloy. Compd.* **2022**, *893*, 162264. [CrossRef]
90. Liu, Z.; He, B.; Lyu, T. A review on additive manufacturing of titanium alloys for aerospace applications: Directed energy deposition and beyond Ti-6Al-4V. *JOM* **2021**, *73*, 1804–1818. [CrossRef]
91. Ren, Y.; Lin, X.; Zeng, Y.; Peng, H.; Huang, W. Long fatigue crack growth behavior of Ti–6Al–4V produced via high-power laser directed energy deposition. *Mater. Sci. Eng. A* **2021**, *819*, 141392. [CrossRef]
92. Bakre, C.; Nassar, A.R.; Reutzel, E.W.; Lissenden, C.J. Ultrasonic Rayleigh Wave Interrogation of Directed Energy Deposition Ti–6Al–4V Having a Rough Surface. *ASME J. Nondestruct. Eval.* **2022**, *5*, 031008. [CrossRef]
93. Li, S.; Kumar, P.; Chandra, S. Directed energy deposition of metals: Processing, microstructures, and mechanical properties. *Int. Mater. Rev.* **2022**, 1–43. [CrossRef]
94. Singh, A.; Kapil, S.; Das, M. A comprehensive review of the methods and mechanisms for powder feedstock handling in directed energy deposition. *Addit. Manuf.* **2020**, *35*, 101388. [CrossRef]
95. Heigel, J.; Michaleris, P.; Reutzel, E. Thermo-mechanical model development and validation of directed energy deposition additive manufacturing of Ti–6Al–4V. *Addit. Manuf.* **2015**, *5*, 9–19. [CrossRef]
96. Lia, F.; Park, J.; Tressler, J. Partitioning of laser energy during directed energy deposition. *Addit. Manuf.* **2017**, *18*, 31–39. [CrossRef]
97. Shim, D.; Baek, G.; Seo, J. Effect of layer thickness setting on deposition characteristics in direct energy deposition (DED) process. *Opt. Laser Technol.* **2016**, *86*, 69–78. [CrossRef]
98. Mahmoud, D.; Elbestawi, M. Lattice Structures and Functionally Graded Materials Applications in Additive Manufacturing of Orthopedic Implants: A Review. *J. Manuf. Mater. Process.* **2017**, *1*, 13. [CrossRef]
99. Tilton, M.; Lewis, G.S.; Bok Wee, H.; Armstrong, A.; Hast, M.W.; Manogharan, G. Additive Manufacturing of Fracture Fixation Implants: Design, Material Characterization, Biomechanical Modeling and Experimentation. *Addit. Manuf.* **2020**, *33*, 101137. [CrossRef]
100. Kuroda, D.; Niinomi, M. Design and Mechanical Properties of New β Type Titanium Alloys for Implant Materials. *Mater. Sci. Eng. A* **1998**, *243*, 244–249. [CrossRef]
101. Huiskes, R.; Weinans, H.; Van Rietbergen, B. The relationship between stress shielding and bone resorption around total hip stems and the effects of flexible materials. *Clin. Orthop. Rel. Res.* **1992**, *274*, 124–134. [CrossRef]
102. Wieding, J.; Wolf, A.; Bader, R. Numerical optimization of open-porous bone scaffold structures to match the elastic properties of human cortical bone. *J. Mech. Behav. Biomed. Mater.* **2014**, *37*, 56–68. [CrossRef]
103. Ahmadi, S.; Yavari, S.; Wauthle, R.; Pouran, B.; Schrooten, J.; Weinans, H.; Zadpoor, A. Additively manufactured open-cell porous biomaterials made from six different space-filling unit cells: The mechanical and morphological properties. *Materials* **2015**, *8*, 1871–1896. [CrossRef]
104. Bobbert, F.S.L.; Lietaert, K.; Eftekhari, A.A.; Pouran, B.; Ahmadi, S.M.; Weinans, H.; Zadpoor, A.A. Additively manufactured metallic porous biomaterials based on minimal surfaces: A unique combination of topological, mechanical, and mass transport properties. *Acta Biomater.* **2017**, *53*, 572–584. [CrossRef]
105. Onal, E.; Frith, J.E.; Jurg, M.; Wu, X.; Molotnikov, A. Mechanical Properties and in Vitro Behavior of Additively Manufactured and Functionally Graded Ti6Al4V Porous Scaffolds. *Metals* **2018**, *8*, 200. [CrossRef]
106. Bai, L.; Gong, C.; Chen, X.; Sun, Y.; Zhang, J.; Cai, L.; Zhu, S.; Xie, S.Q. Additive Manufacturing of Customized Metallic Orthopedic Implants: Materials, Structures, and Surface Modifications. *Metals* **2019**, *9*, 1004. [CrossRef]
107. An, L.; Wang, D.; Zhu, D. Combined Electrochemical and Mechanical Polishing of Interior Channels in Parts Made by Additive Manufacturing. *Addit. Manuf.* **2022**, *51*, 102638. [CrossRef]
108. Ozdemir, Z.; Ozdemir, A.; Basim, G.B. Application of Chemical Mechanical Polishing Process on Titanium Based Implants. *Mater. Sci. Eng. C* **2016**, *68*, 383–396. [CrossRef] [PubMed]
109. Shi, W.; Li, J.; Yuan, M.; Li, Q.; Liu, Y.; Lin, Y. Experimental Study on the Influence Mechanism of Micro-Abrasive Air Jet Machining on the Surface Quality of Ti-6Al-4V Titanium Alloy Formed by Selective Laser Melting. *Mater. Today Commun.* **2022**, *33*, 104429. [CrossRef]
110. Kumar, S.; Prasad, R. Basic principles of additive manufacturing: Different additive manufacturing technologies. In *Additive Manufacturing*; Woodhead Publishing: Cambridge, UK, 2021; pp. 17–35.
111. Bhardwaj, T.; Shukla, M.; Paul, C. Direct energy deposition-laser additive manufacturing of titanium-molybdenum alloy: Parametric studies, microstructure and mechanical properties. *J. Alloy. Compd.* **2019**, *787*, 1238–1248. [CrossRef]
112. Fan, Z. *Study on the Structural Properties of Titanium Alloy Gradient Porous Bionic Bone by Selective Laser Melting*; Chongqing University: Chongqing, China, 2021.
113. Van Hooreweder, B.; Lietaert, K.; Neirinck, B.; Lippiatt, N.; Wevers, M. CoCr F75 scaffolds produced by additive manufacturing: Influence of chemical etching on powder removal and mechanical performance. *J. Mech. Behav. Biomed. Mater.* **2017**, *70*, 60–67. [CrossRef] [PubMed]

114. Bagherifard, S.; Hickey, D.J.; de Luca, A.C.; Malheiro, V.N.; Markaki, A.E.; Guagliano, M.; Webster, T.J. The influence of nanostructured features on bacterial adhesion and bone cell functions on severely shot peened 316L stainless steel. *Biomaterials* **2015**, *73*, 185–197. [CrossRef]
115. Zebrowski, R.; Walczak, M.; Klepka, T.; Pasierbiewicz, K. Effect of the shot peening on surface properties of ti-6al-4v alloy produced by means of DMLS technology. *Eksploat. Niezawodn.* **2019**, *21*, 46–53. [CrossRef]
116. Ma, C.; Andani, M.T.; Qin, H.; Moghaddam, N.S.; Ibrahim, H.; Jahadakbar, A.; Amerinatanzi, A.; Ren, Z.; Zhang, H.; Doll, G.L.; et al. Improving surface finish and wear resistance of additive manufactured nickel-titanium by ultrasonic nano-crystal surface modification. *J. Mater. Process. Technol.* **2017**, *249*, 433–440. [CrossRef]
117. Wu, J. Effect of semi-automatic ultrasonic cleaner on cleaning medical devices. *Med. Equip.* **2018**, *31*, 65–66.
118. Tan, W.X.; Tan, K.W.; Tan, K.L. Developing high intensity ultrasonic cleaning (HIUC) for post-processing additively manufactured metal components. *Ultrasonics* **2022**, *126*, 106829. [CrossRef]
119. Łyczkowska, E.; Szymczyk, P.; Dybała, B. Chemical polishing of scaffolds made of Ti-6Al-7Nb alloy by additive manufacturing. *Arch. Civ. Mech. Eng.* **2014**, *14*, 586–594. [CrossRef]
120. Wang, Y.; Wu, Z.; Zhao, Y. The effect of nonionic surfactants on the cleaning of aluminum alloy after polishing under the synergistic effect of ultrasound. *J. Shanghai Jiao Tong Univ.* **2018**, *52*, 582–586.
121. Vayre, B.; Vignat, F.; Villeneuve, F. Identification on some design key parameters for additive manufacturing: Application on electron beam melting. *Procedia CIRP* **2013**, *7*, 264–269. [CrossRef]
122. Uhlmann, E. Flexible manufacturing with an additive process chain design, production and surface finish. In Proceedings of the ASPE Spring Topical Meeting—Achieving Precision Tolerances in Additive Manufacturing (Proceedings), Raleigh, NC, USA, 26–29 April 2015.
123. Adam, G.; Zimmer, D. On design for additive manufacturing: Evaluating geometrical limitations. *Rapid Prototyp.* **2015**, *21*, 662–670. [CrossRef]
124. Moon, S.; Ma, R.; Attardo, R. Impact of surface and pore characteristics on fatigue life of laser powder bed fusion Ti–6Al–4V alloy described by neural network models. *Sci. Rep.* **2021**, *11*, 20424. [CrossRef]
125. Máša, V.; Horňák, D.; Petrilák, D. Industrial use of dry ice blasting in surface cleaning. *J. Clean. Prod.* **2021**, *329*, 129630. [CrossRef]
126. Axmann, B.; Elbing, F. Strahlverfahren. *Z. Für Wirtsch. Fabr. ZWF* **1997**, *92*, 76–77.
127. Hoenig, S. Cleaning surfaces with dry ice. *Compress. Air Mag.* **1986**, 22–25.
128. Sherman, R. Carbon dioxide snow cleaning. *Part. Technol.* **2007**, *25*, 37–57. [CrossRef]
129. Toscano, T.; Ahmadi, G. Particle removal mechanisms in cryogenic surface cleaning. *Adhesion* **2003**, *79*, 175–201. [CrossRef]
130. Liu, Y.; Hirama, D.; Matsusaka, S. Particle removal process during application of impinging dry ice jet. *Powder Technol.* **2012**, *217*, 607–613. [CrossRef]
131. Spitaels, L.; Rivière-Lorphèvre, É.; Díaz, M. Surface finishing of EBM parts by (electro-) chemical etching. *Procedia CIRP* **2022**, *108*, 112–117. [CrossRef]
132. Surmeneva, M.; Khrapov, D.; Prosolov, K. The influence of chemical etching on porous structure and mechanical properties of the Ti6AL4V Functionally Graded Porous Scaffolds fabricated by EBM. *Mater. Chem. Phys.* **2022**, *275*, 125217. [CrossRef]
133. Buhl, L.; Drue, S.; Lind, L. *Field Testing of Acoustical Cleaning of Electrostatic Precipitators*; Technical University of Budapest: Budapest, Hungary, 1995.
134. Gibbs, B.; Seiffert, G.; Maluski, S. Low frequency sonic cleaning of processes involving powdered material, Tenth International Congress on Sound and Vibration. In Proceedings of the Tenth International Congress on Sound and Vibration, Stockholm, Sweden, 7–10 July 2003.
135. Seiffert, G.; Gibbs, B. Removal of charged powder deposits by high intensity low frequency sound: The role of inertial and drag forces. In Proceedings of the 13th International Conference on Sound and Vibration, Vienna, Austria, 2–6 July 2006; pp. 2–6.
136. Predergast, P. *Powder Removal from Internal Cavities of 3D Printed Parts*; Massachusetts Institute of Technology: Cambridge, MA, USA, 1995.
137. Pharmaceutical Industry Standards of China YY/T1809. *Additive Manufacturing for Medical Applications-Verification Methods of Cleaning and Cleaning Effectiveness of Metal Powder Used in Powder-Bed Fusion Process*; State Drug Administration of China: Beijing, China, 2021.
138. Schllephake, H.; Lehmann, H.; Kunz, U. Ultrastructural findings in soft tissues adjacent to titanium plates used in jaw fracture treatment. *Int. J. Oral Maxillofac. Surg.* **1993**, *22*, 20–25. [CrossRef] [PubMed]
139. Hasib, H.; Harrysson, O.; West, A. Powder removal from Ti-6Al-4V cellular structures fabricated via electron beam melting. *JOM* **2015**, *67*, 639–646. [CrossRef]
140. Liu, Y.; Guo, J.; Shi, W. Study on mechanical properties of 316L stainless steel porous structure by laser powder bed forming. *Chin. J. Lasers* **2022**, *49*, 0802018.
141. Wingham, J.; Turner, R.; Shepherd, J. Micro-CT for analysis of laser sintered micro-composites. *Rapid Prototyp. J.* **2020**, *26*, 649–657. [CrossRef]
142. Hunter, L.; Brackett, D.; Brierley, N. Assessment of trapped powder removal and inspection strategies for powder bed fusion techniques. *Int. J. Adv. Manuf. Technol.* **2020**, *106*, 4521–4532. [CrossRef]

143. Wong, P.-C.; Song, S.-M.; Tsai, P.-H.; Nien, Y.-Y.; Jang, J.S.-C.; Cheng, C.-K.; Chen, C.-H. Relationship between the Surface Roughness of Biodegradable Mg-Based Bulk Metallic Glass and the Osteogenetic Ability of MG63 Osteoblast-like Cells. *Materials* **2020**, *13*, 1188. [CrossRef]
144. Damiati, L.; Eales, M.G.; Nobbs, A.H.; Su, B.; Tsimbouri, P.M.; Salmeron-Sanchez, M.; Dalby, M.J. Impact of Surface Topography and Coating on Osteogenesis and Bacterial Attachment on Titanium Implants. *J. Tissue Eng.* **2018**, *9*, 492–495. [CrossRef]
145. Zhang, X.; Fang, G.; Zhou, J. Additively manufactured scaffolds for bone tissue engineering and the prediction of their mechanical behavior: A review. *Materials* **2017**, *10*, 50. [CrossRef] [PubMed]
146. Arabnejad, S.; Johnston, B.; Tanzer, M.; Pasini, D. Fully porous 3D printed titanium femoral stem to reduce stress-shielding following total hip arthroplasty. *J. Orthop. Res.* **2017**, *35*, 1774–1783. [CrossRef] [PubMed]
147. He, Y.; Zhang, Y.; Shen, X. The fabrication and in vitro properties of antibacterial polydopamine-LL-37-POPC coatings on micro-arc oxidized titanium. *Colloids Surf. B Biointerfaces* **2018**, *170*, 54–63. [CrossRef] [PubMed]
148. Han, W.; Danmei, Z. Study on subchronic systemic toxicity of 3D printed orthopedic titanium alloy. *J. Tissue Eng. Reconstr. Surg.* **2020**, *16*, 6–10.
149. Brydone, A.; Meek, D.; Maclaine, A.S. Bone grafting, orthopaedic biomaterials, and the clinical need for bone engineering. *Proc. Inst. Mech. Eng.* **2010**, *224*, 1329–1343. [CrossRef]
150. Murr, L.E. Open-Cellular Metal Implant Design and Fabrication for Biomechanical Compatibility with Bone Using Electron Beam Melting. *Mech. Behav. Biomed. Mater.* **2017**, *76*, 164–177. [CrossRef]
151. Ameen, W.; Al-Ahmari, A.; Mohammed, M. Design, finite element analysis (FEA), and fabrication of custom titanium alloy cranial implant using electron beam melting additive manufacturing. *Adv. Prod. Eng. Manag.* **2018**, *13*, 267–278. [CrossRef]
152. Mazzoli, A.; Germani, M.; Raffaeli, R. Direct fabrication through electron beam melting technology of custom cranial implants designed in a PHANToM-based haptic environment. *Mater. Des.* **2009**, *30*, 3186–3192. [CrossRef]
153. Zhao, X.; Li, K.; Bai, X. Study on impact resistance of 3D printed titanium alloy personalized skull prosthesis. *Integr. Technol.* **2022**, *11*, 48–56.
154. Tian, K.; Wang, L.; Wang, M.; Li, H.; Chen, R.; Zhang, K. Experimental study of 3D printed porous titanium scaffolds loaded with BMP-2 and VEGF for jaw defect repair. *Beijing Stomatol.* **2022**, *30*, 165–170.
155. Yan, R.; Luo, D.; Huang, H.; Li, R.; Yu, N.; Liu, C.; Hu, M.; Rong, Q. Electron beam melting in the fabrication of three-dimensional mesh titanium mandibular prosthesis scaffold. *Sci. Rep.* **2018**, *8*, 1–10. [CrossRef] [PubMed]
156. Moiduddin, K.; Hammad, M.; Umer, U. Reconstruction of complex zygomatic bone defects using mirroring coupled with EBM fabrication of titanium implant. *Metals* **2019**, *9*, 1250. [CrossRef]
157. Mommaerts, M.Y. Additively Manufactured Sub-Periosteal Jaw Implants. *Int. J. Oral Maxillofac. Surg.* **2017**, *46*, 938–940. [CrossRef] [PubMed]
158. Van den Borre, C.; Rinaldi, M.; De Neef, B. Patient-and clinician-reported outcomes for the additively manufactured sub-periosteal jaw implant (AMSJI) in the maxilla: A prospective multicentre one-year follow-up study. *Int. J. Oral Maxillofac. Surg.* **2022**, *51*, 243–250. [CrossRef] [PubMed]
159. Vos, T.; Allen, C.; Arora, M.; Barber, R.; Bhutta, Z.; Brown, A. Global, regional, and national incidence, prevalence, and years lived with disability for 310 diseases and injuries, 1990–2015: A systematic analysis for the Global Burden of Disease Study 2015. *Lancet* **2016**, *388*, 1545–1602. [CrossRef]
160. Bosshardt, D.D.; Chappuis, V.; Buser, D. Osseointegration of titanium, titanium alloy and zirconia dental implants: Current knowledge and open questions. *Periodontology* **2017**, *73*, 22–40. [CrossRef]
161. Wang, H.; Wang, Y.; Zhang, B. Cytotoxicity of 3D printed titanium alloy dental implants. *Chin. J. Oral Implantol.* **2019**, *24*, 10–13.
162. Tolochko, N.; Savich, V.; Laoui, T. Dental root implants produced by the combined selective laser sintering/melting of titanium powders. *J. Mater. Des. Appl.* **2002**, *216*, 267–270. [CrossRef]
163. Chan, K.; Koike, M.; Mason, R. Fatigue life of titanium alloys fabricated by additive layer manufacturing techniques for dental implants. *Metall. Mater. Trans. A* **2013**, *44*, 1010–1022. [CrossRef]
164. Gonzalez, J.; Mirza-Rosca, J. Study of the corrosion behavior of titanium and some of its alloys for biomedical and dental implant applications. *J. Electroanal. Chem.* **1999**, *471*, 109–115. [CrossRef]
165. Hamza, H.M.; Deen, K.M.; Haider, W. Microstructural Examination and Corrosion Behavior of Selective Laser Melted and Conventionally Manufactured Ti6Al4V for Dental Applications. *Mater. Sci. Eng. C* **2020**, *113*, 110980. [CrossRef] [PubMed]
166. Zhou, H.; Fan, Q. 3D re-construction and SLM survey for dental implants. *Mech. Med. Biol.* **2017**, *17*, 1750084. [CrossRef]
167. Takemoto, M.; Fujibayashi, S.; Neo, M.; So, K.; Akiyama, N.; Matsushita, T.; Kokubo, T.; Nakamura, T. A Porous Bioactive Titanium Implant for Spinal Interbody Fusion: An Experimental Study Using a Canine Model. *J. Neurosurg. Spine* **2007**, *7*, 435–443. [CrossRef]
168. Wu, S.-H.; Li, Y.; Zhang, Y.-Q.; Li, X.-K.; Yuan, C.-F.; Hao, Y.-L.; Zhang, Z.-Y.; Guo, Z. Porous Titanium-6 Aluminum-4 Vanadium Cage Has Better Osseointegration and Less Micromotion than a Poly-Ether-Ether-Ketone Cage in Sheep Vertebral Fusion. *Artif. Organs* **2013**, *37*, 191–201. [CrossRef] [PubMed]
169. Hollander, D.A.; Von Walter, M.; Wirtz, T.; Sellei, R.; Schmidt-Rohlfing, B.; Paar, O.; Erli, H.J. Structural, mechanical and in vitro characterization of individually structured Ti-6Al-4V produced by direct laser forming. *Biomaterials* **2006**, *27*, 955–963. [CrossRef]
170. Lin, C.-Y.; Wirtz, T.; LaMarca, F.; Hollister, S.J. Structural and Mechanical Evaluations of a Topology Optimized Titanium Interbody Fusion Cage Fabricated by Selective Laser Melting Process. *J. Biomed. Mater. Res. Part A* **2007**, *83A*, 272–279. [CrossRef]

171. Xu, N.; Wei, F.; Liu, X.; Jiang, L.; Cai, H.; Li, Z.; Yu, M.; Wu, F.; Liu, Z. Reconstruction of the upper cervical spine using a personalized 3D-printed vertebral body in an adolescent with ewing sarcoma. *Spine* **2016**, *41*, E50–E54. [CrossRef] [PubMed]
172. Fujibayashi, S.; Takemoto, M.; Neo, M.; Matsushita, T.; Kokubo, T.; Doi, K.; Ito, T.; Shimizu, A.; Nakamura, T. A Novel Synthetic Material for Spinal Fusion: A Prospective Clinical Trial of Porous Bioactive Titanium Metal for Lumbar Interbody Fusion. *Eur. Spine J.* **2011**, *20*, 1486–1495. [CrossRef] [PubMed]
173. Turna, A.; Kavakli, K.; Sapmaz, E.; Arslan, H.; Caylak, H.; Gokce, H.S.; Demirkaya, A. Reconstruction with a Patient-Specific Titanium Implant after a Wide Anterior Chest Wall Resection. *Interdiscip. CardioVascular Thorac. Surg.* **2013**, *18*, 234–236. [CrossRef]
174. Alvarez, A.; Evans, P.; Dovgalski, L. Design, additive manufacture and clinical application of a patient-specific titanium implant to anatomically reconstruct a large chest wall defect. *Rapid Prototyp. J.* **2021**, *27*, 304–310. [CrossRef]
175. Goldsmith, I.; Evans, P.; Goodrum, H. Chest wall reconstruction with an anatomically designed 3-D printed titanium ribs and hemi-sternum implant. *3D Print. Med.* **2020**, *6*, 1–7. [CrossRef] [PubMed]
176. Liu, Y.; Zhang, J.; Zhang, Y.; Lin, Q.; Wu, H.; Xu, Q.; Chen, L. The application of 3D printed titanium alloy artificial ribs and autologous rib transplantation in partial resection of ribs and sternoclavicular. *Jiangxi Med.* **2021**, *56*, 31–33+36.
177. Fang, C.; Cai, H.; Kuong, E. Surgical applications of three-dimensional printing in the pelvis and acetabulum: From models and tools to implants. *Der Unf.* **2019**, *122*, 278–285. [CrossRef] [PubMed]
178. Zhu, Y.; Babazadeh-Naseri, A.; Dunbar, N. Finite Element Analysis of Screw Fixation Durability under Multiple Boundary and Loading Conditions for a Custom Pelvic Implant. *Med. Eng. Phys.* **2022**, *11*, 103930. [CrossRef]
179. Wong, K.C.; Kumta, S.M.; Gee, N.V.L.; Demol, J. One-step reconstruction with a 3D-printed, biomechanically evaluated custom implant after complex pelvic tumor resection. *Comput. Aided Surg.* **2015**, *20*, 14–23. [CrossRef]
180. Broekhuis, D.; Boyle, R.; Karunaratne, S. Custom designed and 3D-printed titanium pelvic implants for acetabular reconstruction after tumour resection. *HIP Int.* **2022**, *11*, 11207000221135068. [CrossRef] [PubMed]
181. Park, J.W.; Park, H.; Kim, J.H.; Kim, H.M.; Yoo, C.H.; Kang, H.G. Fabrication of a Lattice Structure with Periodic Open Pores through Three-Dimensional Printing for Bone Ingrowth. *Sci. Rep.* **2022**, *12*, 17223. [CrossRef]
182. Lv, Y.; Wang, B.; Liu, G.; Tang, Y.; Liu, J.; Wei, G.; Wang, L. Design of Bone-like Continuous Gradient Porous Scaffold Based on Triply Periodic Minimal Surfaces. *J. Mater. Res. Technol.* **2022**, *21*, 3650–3665. [CrossRef]
183. Gupta, S.K.; Shahidsha, N.; Bahl, S.; Kedaria, D.; Singamneni, S.; Yarlagadda, P.K.D.V.; Suwas, S.; Chatterjee, K. Enhanced Biomechanical Performance of Additively Manufactured Ti-6Al-4V Bone Plates. *J. Mech. Behav. Biomed. Mater.* **2021**, *119*, 104552. [CrossRef]
184. Scherer, K.; Huwer, A.; Ulber, R.; Wahl, M. Optimizing Luminous Transmittance of a Three-Dimensional-Printed Fixed Bed Photobioreactor. *3D Print. Addit. Manuf.* **2022**. [CrossRef]
185. Weißmann, V.; Boss, C.; Schulze, C.; Hansmann, H.; Bader, R. Experimental characterization of the primary stability of acetabular press-fit cups with open-porous load-bearing structures on the surface layer. *Metals* **2018**, *8*, 839. [CrossRef]
186. Murr, L.E.; Amato, K.N.; Li, S.J.; Tian, Y.X.; Cheng, X.Y.; Gaytan, S.M.; Martinez, E.; Shindo, P.W.; Medina, F.; Wicker, R.B. Microstructure and mechanical properties of open-cellular biomaterials prototypes for total knee replacement implants fabricated by electron beam melting. *J. Mech. Behav. Biomed. Mater.* **2011**, *4*, 1396–1411. [CrossRef] [PubMed]
187. Herbert, N.; Simpson, D.; Spence, W.; Ion, W. A preliminary investigation into the development of 3D printing of prosthetic sockets. *Rehabil. Res. Dev.* **2005**, *42*, 141–146. [CrossRef] [PubMed]
188. Zuniga, J.M.; Dimitrios, K.; Peck, L.; Srivastava, R.; Pierce, J.E.; Dudley, D. Coactivation index of children with congenital upper limb reduction deficiencies before and after using a wrist-driven 3D printed partial hand prosthesis. *J. Neuroeng. Rehabil.* **2018**, *15*, 48. [CrossRef] [PubMed]
189. Telfer, S.; Pallari, J.; Munguia, J.; Dalgarno, K.; McGeough, M.; Woodburn, J. Embracing additive manufacture: Implications for foot and ankle orthosis design. *BMC Musculoskelet. Disord.* **2012**, *13*, 84. [CrossRef]
190. Paterson, A.; Bibb, R.; Campbell, R.; Bingham, G. Comparing additive manufacturing technologies for customised wrist splints. *Rapid Prototyp.* **2015**, *21*, 230–243. [CrossRef]